International Journal of Environmental Sciences
ISSN: 2229-7359
Vol. 11 No. 8, 2025
https://www.theaspd.com/ijes.php

Thermoelectric Heat Pump (TE) Drying System Simulation And Performance Analysis For Tomatoes

Mohamed Ibrahim El Didamony [1]*, Shimaa Elsaid Salah[2], Abeer Wagdy Elhaddad[3], Mohamed Saied Ghoname[4]

[1]Agricultural Engineering Department, Faculty of Agriculture, Tanta University, Egypt; el-didamony@agr.tanta.edu.eg

[2]Agricultural Engineering Department, Faculty of Agriculture, Tanta University, Egypt; shimaa.salah@agr.tanta.edu.eg

Researcher at agricultural engineering research institute, Power and energy department, Egypt abeer_wz3000@yahoo.com

[4]Agricultural Engineering Department, Faculty of Agriculture, Tanta University, Egypt; mohamed.ghonaim@agr.tanta.edu.eg

Abstract: *The main aim of the study was to preserve and dry the tomato crop to keep it for a long time and be easy to preserve, transport, and maintain its quality. By manufacturing a fast-drying and continuous drying chamber that preserves the tomatoes' quality and their nutrient. The effect of using Peltier in drying tomato slices was investigated at three thicknesses (0.5, 1 and 1.5 cm), on some thermodynamic parameters (Drying rate, Energy consumption for dried sliced tomato (ET), Specific energy consumption (Esp), Specific energy consumption (SEC) and Energy Efficiency (η_E) and chemical characterization of tomato (lycopene, β – carotene and antioxidant activity) under using four air velocities (0.5, 1.5, 2 and 2.5 cm) at three-outlet fan area of (20, 40 and 60 cm^2). A Simulation analysis using ANSYS was done to study the distribution of drying airflow inside the drying chamber in different cases (when no fans are used, with a fan at the outlet only, with only two small fans inside the drying chamber, and with a fan at the outlet and two small fans inside the drying chamber at different air velocities (0.5, 1.5, 2 and 2.5 m s^{-1}) and different fan outlet areas (20, 40 and 60 cm^2). Experimental data showed that the energy consumption varied between 0.42 and 2.49 kWh; whereas (E_{sp}) varied between 0.43 kWh kg^{-1} of initial mass and 2.54 kWh kg^{-1} of initial mass, and SEC varied between 0.57 kWh kg^{-1} of moisture removed and 6.26 kWh kg^{-1}. Energy efficiency (η_E) of sliced tomato samples ranged between* $10.66 \leq \eta_E \leq 63.39\%$ *. The maximum η_E value was obtained at 0.5 cm slice thickness, 0.5 m s^{-1} and 20 cm^2 outlet fan area treatment combination. The maximum values of lycopene contents and β-carotene was (52.46 mg/100 gm and 93.35 mg/100 gm) respectively at a slice thickness of 0.5 cm and 0.5 m s^{-1} air velocity, and 20 cm^2 fan outlet area. The maximum antioxidant value was 30.37 % at a tomato slice thickness of 1.5 cm and air velocity (2.5 m s^{-1}) at a fan outlet area of 60 cm^2*

Keywords: *Peltier; Drying; Energy required; Tomato; Simulation; Thermoelectric; TE; Heat Pump.*

1. INTRODUCTION

Tomatoes hold significant importance as a strategic crop globally, serving essential functions across different industries despite their tendency to spoil quickly. To combat this issue and prolong their freshness, drying has emerged as a popular preservation method for these perishable products. This age-old technique not only helps in maintaining the quality of tomatoes but also offers an alternative approach for preparing and enjoying these crops for future use (Tang et al., 2025). Dehydration, often referred to as drying, is a method of food preservation that eliminates moisture. This not only enhances the stability of the food for storage but also reduces the weight for transportation and minimizes packaging requirements. The drying process plays a crucial role in determining the final product's quality, affecting its nutritional value, appearance, taste, and level of shrinkage (Botelho et al., 2025). Therefore, it should be done in a way that will be least detrimental to the product quality

The tomato (Lycopersicon esculentum L.) is a popular vegetable, known for how easily it spoils and its seasonal growth cycles. It's grown and enjoyed in many countries around the globe. Recent reports indicate that tomatoes are the second most cultivated crop, following potatoes, in terms of both growing area and overall production.(Monday John et al., 2020). The national Egyptian production of tomatoes was 6211015.96 tonnes in 2023, according to the (FAO, 2025). Tomatoes are a seasonal crop characterized by their high content of lycopene, β-carotene, phenolic compounds, and ascorbic acid (Perveen et al., 2015). The main phytochemical found in tomatoes is lycopene, a vibrant red pigment that becomes more concentrated as the fruit ripens. In addition to lycopene, tomatoes are rich in other carotenoids such as phytoene and phytofluene. They also boast phenolic compounds, including coumaric

acid, chlorogenic acid, and various flavonoids like quercetin and rutin (Lister et al., 2005). Tomatoes are a highly perishable food that begins to deteriorate within 2–3 days after harvest (Ochida et al., 2018). The quality of tomatoes is primarily evaluated based on their weight, color, firmness, and flavor (Mai Al-Dairi, 2021).

Tomatoes are climacteric fruits, and their physiological characteristics make them highly delicate agricultural commodities (Chero et al., 2021).It is well established that tomatoes can be affected by post-harvest factors, including storage conditions, handling, and transportation (Wu & Wang, 2014). Besides, (Kipchumba Cherono, Milindi Sibomana, 2018) . Post-harvest losses in tomatoes can soar to as much as 40%. The quality of agricultural products is crucial for both consumers and producers alike. While fresh tomatoes offer the greatest nutritional benefits, their high moisture content—around 94%—renders them highly perishable (Zalewska et al., 2022), Ripe tomatoes tend to spoil rapidly, creating a notable hurdle for growers, especially since they are an annual crop. This underscores the critical need for effective storage solutions. Additionally, thermal processing can affect the tomatoes' color, sensory characteristics, nutritional benefits, and overall quality (Cernîşev, 2010) .

From an energy standpoint, convective hot-air drying has a significant downside: it takes a long time to dry and operates at high temperatures, leading to considerable energy usage—potentially hitting as much as 6,000 kJ for every kilogram of water evaporated (Mujumdar & Menon, 2020) . To improve the retention of tomato quality, many researchers have pointed to the benefits of using such dryers. Nonetheless, this dehydration method tends to demand a significant amount of energy. This is primarily due to the lower energy efficiency of convective crop dryers when compared to other artificial drying systems, as well as the limited thermal conductivity that occurs during the falling rate stage of the drying process (Beigi, 2016). Since evaporated water possesses a high latent heat capacity, it limits heat transfer by convection to the food matrix (Motevali et al., 2016) ; and (Nwakuba et al., 2016). (Darvishi, 2013) organoleptic considerations should be applied in a manner that minimizes changes to the quality of the dried product. (Minaei et al., 2014) to lower energy usage, several drying techniques are utilized for dehydrating products. These techniques include microwave drying, heat pump drying (HPD), infrared drying, and freeze-drying (FD). Recently, microwave drying has gained popularity for drying apples along with other fruits and vegetables (Chong et al., 2014) and carrots (Arikan et al., 2012). Microwave energy provides several advantages over conventional heating methods, including faster operation, reduced energy consumption, precise process control, and shorter start-up and shutdown times (Botha et al., 2012). Microwave drying offers several advantages, including selective heating, high energy efficiency, rapid processing, and reduced floor space requirements. It is not only faster but also consumes less energy than conventional drying methods (Schiffmann, 2001). Microwave power plays a crucial role in the drying process. Using low power can result in lower temperatures and a slower drying rate, while too much power might create excessively high temperatures and uneven energy distribution, ultimately affecting the quality of the final product. Despite these considerations, microwave drying has proven effective for a variety of food materials (Arslan & Özcan, 2011) . Increasing the microwave power during the final drying stage of banana slices has been found to accelerate the drying rate, thereby reducing the total drying time (Sousa et al., 2004). Excessive microwave power can cause a rapid rise in the product's temperature, leading to charring—a phenomenon known as temperature runaway. Therefore, it is essential to regulate microwave power during the final drying stage to prevent temperature runaway and maintain product quality. While solar food drying is widely practiced, the drying rate is influenced by several factors, particularly sunlight intensity and relative humidity. Depending on sunlight availability, airflow, humidity levels, and the type of food being dried, solar dryers typically require 1 to 3 days to complete the process.

Based on what we've talked about, it's clear that these systems use a lot of energy and can be expensive to run. Fortunately, technology utilizing the Peltier effect is showing promise as a possible solution to this problem.The Peltier system is an energy-efficient heating method and environmentally friendly due to its low power consumption (Fatouh et al., 2006). When a heat pump system is paired with a dryer, it's often

called a heat pump dehumidifier or a heat pump dehydrator. In a Peltier device, the flow of electrical current decides whether the unit will cool or heat by moving heat from one side to the other. This technology, which includes terms like Peltier heat pump, solid-state refrigerator, or thermoelectric cooler (TEC), is versatile enough for both heating and cooling needs.(Taylor & Solbrekken, 2008). Thermoelectric (TE) heat pumps are just one of the various ways TE modules can be utilized, yet research in this field is still quite scarce. Among the limited studies published, one notable example focuses on the design and testing of a TE-based clothes dryer (Liu et al., 2008). Their findings indicated that the drying rate decreases over time and is strongly influenced by the temperature difference between the hot and cold sides of the TE modules. A mathematical model was also developed for a TE heat pump recuperative system designed for a dryer (Patel et al., 2018). The model integrated various factors such as temperature-dependent material properties, contact resistance, and both thermal and electrical resistance. A prototype thermoelectric heat exchanger was constructed and put through testing, yielding experimental data that confirmed the model's accuracy. This model can now be utilized to forecast the performance of a thermoelectric heat pump in a convection tumble dryer.

While TE drying systems aren't a novel concept in energy technology, their effectiveness in production is still up for discussion. Important metrics to consider include thermal performance, total energy usage, energy efficiency, specific energy consumption, and the overall economic cost of the drying process. These aspects ultimately shape the reliability of the system as a drying solution. Given the nutritional significance of tomatoes, it's essential to understand how the drying process affects their quality. Additionally, the demand for low-energy drying methods and the lack of thorough studies on TE technology's impact on the qualitative and thermodynamic characteristics of tomatoes highlight the need for further research. In Egypt, solar drying stands out as the main technique for preserving agricultural products. However, it often struggles to maintain the high quality of these goods. Its performance can be further hampered by the need for consistent sunlight, which isn't always available. Moreover, solar dryers are not ideal for areas that experience limited sunlight or cold weather conditions. This challenge inspired the creation of a dryer that can generate consistent heat while using minimal energy, enhancing the drying process and maintaining the quality of different agricultural products.

This study focuses on simulating a drying system that utilizes a thermoelectric heat pump (TE) and aims to explore its impact on the quality of tomato slices, the kinetics of the drying process, and overall energy consumption. The primary goals are: (1) To investigate how different outlet fan velocity (0.5, 1.5, 2.0, and 2.5 m/s), varying outlet hole sizes (20, 40, and 60 cm^2), and tomato slice thicknesses (0.5, 1.0, and 1.5 cm) affect the drying dynamics, as well as to compare two different drying models; (2) To evaluate the effectiveness of the designed dryer by measuring key performance indicators such as heating capacity (Qh), coefficient of performance (COP), specific energy consumption (SEC), energy efficiency, electrical energy use, and quality metrics of the tomato slices under various conditions, all aimed at identifying the best operating parameters.

2. MATERIALS AND METHODS

The experiments for this study were conducted in El Ibrahimia, Al Sharkia Governorate, Egypt, located at 30.71°N latitude and 31.56°E longitude, during January and February 2023. This section presents the design of the proposed drying system along with construction details, including materials used, dimensions, and insulation. The subsequent sections describe the experimental procedures and the measuring instruments employed.

2.1. Materials

2.1.1. Crop (Tomato)

Tomatoes (Lycopersicon esculentum), which start off with a moisture level of 92% (wet basis), generally start to spoil within 3 to 5 days. To enhance their longevity, we dried them down to about 10% moisture content. For our experiments, we prepared tomato slices in three thicknesses: 0.5 cm, 1 cm, and 1.5 cm, as illustrated in Figure 1.

Figure 1. Fresh tomato (Roma).

2.1.2. Drying unit

The drying unit is made up of five key components: a drying chamber, a heating source (specifically a Thermoelectric Peltier module, model TEC1-12706), recirculation fans, an extraction fan, a power source, and a control unit. The drying chamber has a rectangular shape and features three layers of insulation: a 10 mm thick plywood exterior, 40 mm thick polyurethane in the middle, and a 1 mm stainless-steel interior layer. For the experiments conducted, the internal dimensions of the chamber were 415 mm in length, 300 mm in width, and 395 mm in height, as illustrated in Figure 2.

The unit features three openings. The top one, sized at 230 mm in length and 220 mm in width, accommodates an extraction fan (model N10-20n). This fan operates with a power input of 40 W at AC 220–240 V, running between 1300 and 1550 rpm, and can achieve a maximum airflow rate of 0.1256 m^3/s. The fan speed is automatically controlled by an electronic tap changer, ensuring the air velocity remains optimal.

The two remaining side openings were utilized to install four thermoelectric (TE) modules, specifically the TEC1-12706 model. Each module has the following specifications: an operating voltage of 12 V, a current rating of 6 A, a maximum voltage (Umax) of 15.2 V, a maximum temperature difference (ΔT_{max}) of 67°C, and a maximum power consumption of 70 W. These four thermoelectric heat pumps were connected in series.

The hot-side heat sink featured 15 fins, each measuring 20 cm in length, 7 cm in width, and 5 cm in height from the base, as illustrated in Figure 3. These heat sinks were strategically located at the air inlet of the drying chamber, facing the two recirculation fans placed on the opposite side. Within the drying chamber, two small recirculation fans, each 60 mm in diameter and functioning at 12 V, were mounted on opposite sides, aimed directly at the hot surface of the Peltier unit's heat sink. This configuration ensured an even distribution of hot air over the trays.

The control unit is made up of three key components: a power source, an electronic tap changer to adjust the fan speed, and a temperature controller equipped with an indicator display. The power source utilizes a TWINHA AC voltage transformer (transforming 110V/220V to DC 12V, 30A) in combination with a 350 W switching power supply designed for LED strips (model H10064).

A temperature controller and indicator, model MT-512E, was utilized to monitor and regulate the dryer's temperature, achieving a control range from –50°C to 75°C. At the beginning of the experiments, the sensor underwent calibration. The control system effectively maintained the dryer temperature at a consistent 60°C set point.

International Journal of Environmental Sciences
ISSN: 2229-7359
Vol. 11 No. 8, 2025
https://www.theaspd.com/ijes.php

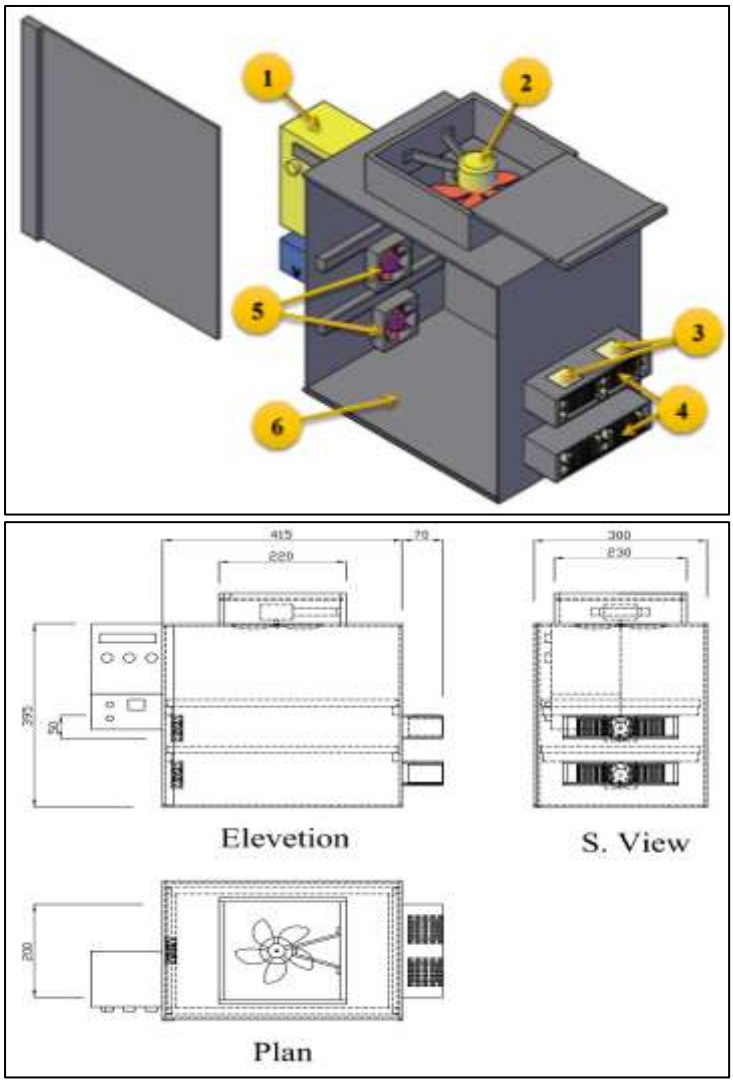

No.	Part name	No.	Part name	No.	Part name
1	Control unit	3	Peltier unit	5	Recirculation fan
2	Extraction fan	4	Heat sink	6	Drying chamber

Figure 2. The schematic diagram for the drying system.

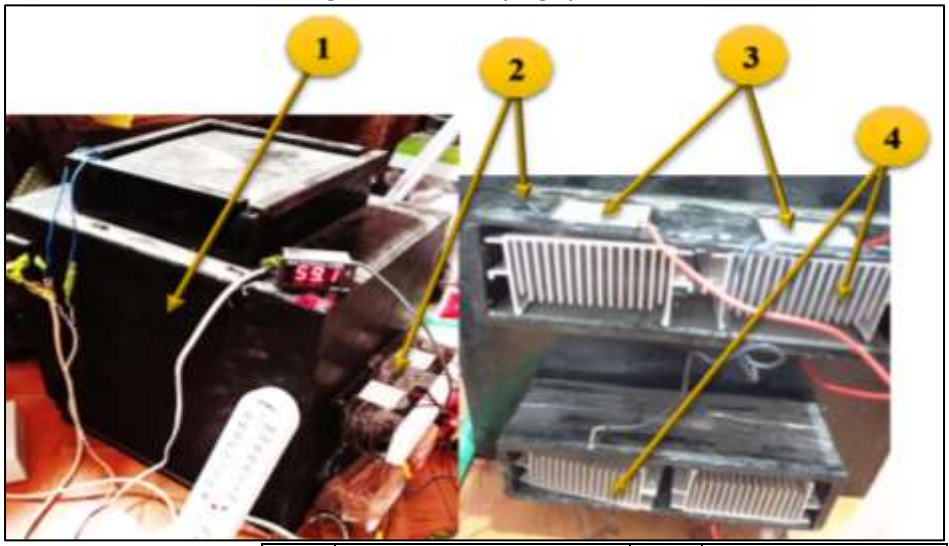

No.	Part name	No.	Part name
1	Drying chamber	3	Peltier unit
2	Heating source unit	4	Heat sink

Figure 3. Heat sink with heating source unit (TE-TEC1-12706).

2.1.3. Preparation of tomato slices

Tomatoes were carefully washed under running water to eliminate any dirt and soil. After draining excess water on a plastic net, they were sorted and sliced into three thicknesses—0.5 cm, 1.0 cm, and 1.5 cm—using a HANDLE RG-400 fruit slicer from Sweden, before the pre-treatment processes.

2.2. Methods

The experiment was conducted in three main stages to construct a drying unit utilizing the thermoelectric Peltier effect for drying fresh tomato slices while preserving their valuable nutritional components:

1. Dryer design (simulation using ANSYS)
2. Experimental setup design
3. Experimental procedure

2.2.1. The dryer design (Simulation using ANSYS)

The main objective of this analysis was to investigate the uniform distribution of drying airflow inside the drying chamber to ensure drying uniformity and achieve near-uniform airflow. The numerical analysis for the present experimental study was carried out using ANSYS 17.2 software and included the following cases:

1. Simulation of the heat sink and thermoelectric Peltier (TE).
2. Simulation of an empty drying chamber without any fan.
3. Simulation of an empty drying chamber with a fan at the outlet only.
4. Simulation of an empty drying chamber with two small fans inside the drying chamber only.
5. Simulation of an empty drying chamber with a fan at the outlet and two small fans inside the drying chamber, analyzed under:

a) Different outlet fan velocities (0.5, 1.5, 2.0, and 2.5 m/s).

b) Different outlet hole areas (20, 40, and 60 cm^2).

The simulation of the heat sink and thermoelectric cooler (TEC) was performed using system coupling between mechanical (steady-state thermal) and fluid flow (Fluent) modules in **ANSYS 17.2 Workbench**. The geometry was created using SolidWorks software. This step aimed to investigate the temperature and heat flux of the heat sink entering the drying chamber for each case.

The boundary conditions for the mechanical (steady-state thermal) analysis were defined as follows: ambient temperature of 32 °C, TEC surface temperature of 70 °C, and heat transfer coefficients for each case ranging from 0.76 to 3.01 $W/m^2 \cdot °C$. The heat sink was made of aluminum, with a thermal conductivity of 202.4 $W/m \cdot K$, a density of 2719 kg/m^3, and a specific heat capacity of 871 $J/kg \cdot °C$ (Hernandez-Perez et al., 2021). The boundary conditions for the fluid flow (Fluent) analysis were defined as follows: energy equation enabled, laminar flow, working fluid set to air (ideal gas), and inlet velocity ranging from 0.1 to 2.5 m/s for each case. For the outlet boundary condition, the gauge pressure was set to zero.

The Computational Fluid Dynamics (CFD) analysis of the drying chamber for each case was performed in Fluent to investigate the temperature and airflow distribution inside the chamber. The geometry was created in SolidWorks, with outlet hole areas varying from 20 to 60 cm^2.

To evaluate the temperature and airflow distribution within the drying chamber, the energy equation was activated. The working fluid was defined as air, and the chamber walls were modeled as wood. Different inlet velocities (0.1 to 2.5 m/s) were tested, with the outlet gauge pressure set to zero in all cases. The following equations were used to calculate the convective heat transfer coefficient and determine the flow regime (laminar or turbulent) (Hammami et al., 2017):-

$$h_c = \frac{Nu \times k}{L} \quad (1)$$

$$Nu = 0.664 \times Re^{\frac{1}{2}} \times Pr^{\frac{1}{3}} \quad (2)$$

$$Re = \frac{\rho \times V \times L}{\upsilon} \quad (3)$$

$$Pr = \frac{\mu \times cp}{k} \quad (4)$$

Where h_c is the convection heat transfer coefficient is Nusselt number, k is thermal conductivity, is 0.02814 W/m.K, L is characteristic length, m, Re is Reynolds number, is the density of the fluid, is 1.0877 kg/m^3, V is the fluid velocity, m s-1, Pr is Prandtl number is air dynamic viscosity, is 1.828×10-5 at 30 °C, Cp is air specific heat, is 1007.4 J/(Kg. K) for dry air and ν is dynamic viscosity/m.s.

2.2.2. Experimental setup design

The tomato dryer, detailed in Section 2.2.1 through Equations (1) to (4), underwent testing in January and February 2023. The experiments assessed three different thicknesses of tomato slices (0.5, 1.0, and 1.5 cm), four varying fan air velocities (0.5, 1.5, 2.0, and 2.5 m/s), and three different outlet areas (20, 40, and 60 cm^2).

2.2.3. Experimental Procedure

Tomatoes were selected with care, thoroughly washed, and then spread out evenly across the three designated trays inside the drying chamber, as illustrated in Fig. 4. Before commencing the experiment, a sample from each tray was weighed. The drying temperature was consistently maintained at 60 °C throughout the drying process, monitored by an Mt 512 E temperature controller and indicator.

Samples were monitored every hour until they reached the desired moisture content. The airflow during the drying process was adjusted based on the treatment conditions, with velocities set at 0.5, 1.5, 2.0, and 2.5 m/s. The drying continued until the balance consistently showed the same sample weight for three consecutive readings, signifying that the final moisture content had been attained.

Fig. 4 Tomato slice distributed inside the drying chamber.

2.2.4. Measurements and Instrumentation

A 16-channel data logger was utilized to gather, document, and analyze measurements from multiple sensors, including L.M. thermistors that have an accuracy of ± 0.25 °C at room temperature. Additionally, measurements from the heat sinks were recorded. Outside the drying unit, two sensors were deployed to measure the dry-bulb temperature ($T_{o,db}$) and the wet-bulb temperature ($T_{o,wb}$). The wet-bulb temperature was obtained by wrapping thermistors in a wet cloth. To determine the indoor relative humidity (RH_i) and outdoor relative humidity (RH_o), a psychometric chart program was employed.

The data logger was set up with a keyboard and monitor. The Lap Jack program was utlized to control the data logger through the computer, while the Profilap software transformed the analog readings into a digital format. Data was collected every five minutes, with integrated measurements taken each minute. All sensors and data loggers underwent calibration before the experiments commenced.

A U.S. Solid balance scale was utilized to weigh the tomato samples, featuring a maximum capacity of 50 kg, a resolution of 0.01 g, and an accuracy of ±0.02 g. To measure the dimensions of the tomato slices, a digital Vernier caliper with an accuracy of ±0.01 mm was employed. Additionally, a digital fan anemometer (Model UNI-UT363) was used to measure the average air velocity at various points inside the dryer and at the axial fan outlets. This model has a range of 0–30 m/s, an accuracy of ±5% of the least significant digit, and a resolution of 0.1 m/s.

The axial fans were calibrated by assessing the airspeed at the outlet, measuring it at six different points throughout the fan's cross-sectional area. The average airspeed was then multiplied by the cross-sectional area to determine the air-flow rate. For monitoring the electrical consumption of the TE modules, we utilized a digital multimeter (Model Total TMT47503) to measure both AC and DC voltage and current. This multimeter provides an accuracy of ±(0.5% of reading + 3) V for voltage and ±(1.2% of reading + 3) A for DC, with a maximum input voltage of 750 V AC.

2.2.5. Calculation

2.2.4. Drying kinetics

Moisture content (M.C$_{db}$,%)

The initial moisture levels of both the fresh and dried materials were measured using Equation (5) along with the atmospheric air oven method, conducted at a temperature of 105 ± 2 °C for a duration of 24 hours.(AOAC, 2023). The moisture content on a wet basis was determined by measuring the difference in mass between the original and dried samples, then expressing this difference as a percentage of the mass of the original sample.

$$MC_{db} = \frac{M_{wet} - M_{dry}}{M_{dry}} \quad (5)$$

Where: MC_{db} is moisture content, dry basis %; M_{wet} is mass of wet samples, g, and M_{dry} is mass of dry samples, g.

Moisture Ratio (MR) and Drying Rate

Equation (6), as reported by (Saha et al., 2019) , was used to calculate the moisture ratio (MR) of tomato slices.

$$MR = \frac{M_t - M_e}{M_o - M_e} \quad (6)$$

Where MR, the moisture ratio, M_t, moisture content at a specific time, %(d. b.). M_o and M_e, initial and equilibrium moisture content % (d.b.).

Drying rate (DR*)*

The drying rate (DR) of tomato fruit was calculated using Eq. (7) (I. Doymaz, 2012).

$$DR = \frac{M_{t+dt} - M_t}{dt} \quad (7)$$

Where: DR is the drying rate ($kg_{water}/kg_{dry\ base}.hr$); M_t is the moisture content ($kg_{water}/kg_{dry\ matter}$) at time (t); M_{t+dt} is, moisture content ($kg_{water}/kg_{dry\ matter}$) at time (t+dt), and dt is drying time,h.

Empirical Drying Models

According to several researchers, the equilibrium moisture content (m_e) is negligible and can be disregarded

(Doymaz, 2004). Consequently, the Lewis model can be expressed as follows:

$$MR = \frac{M_t - M_e}{M_o - M_e} = \exp(-k_L \times t) \quad (8)$$

Where *MR* is the moisture ratio; M_t is the moisture content (% w.b.) at time *t*; M_o is the initial moisture content (% w.b.); M_e is the equilibrium moisture content (% w.b.); and K_L is the Lewis drying constant (min^{-1}).

(Akpinar et al., 2003) introduced a two-term equation proposed by Henderson and Pabis, which can be expressed as:-

$$MR = \frac{M_t - M_e}{M_o - M_e} = \alpha \exp(-k_H \times t) \quad (9)$$

Where α is the drying constant, dimensionless, and K_H is the Henderson drying constant, min^{-1}.

The effectiveness of two mathematical models (Eq. 10 and Eq. 12) for studying the drying process of tomato leather under various conditions was examined using MATLAB software. The drying constants (k_L and k_h) played a critical role in evaluating how well these models fit the observed data.

To assess how well the model fits the data, we used several criteria for selection. These included the reduced chi-square (χ^2), mean bias error (MBE), root mean square error (RMSE), and standard error (SE). Additionally, we took the coefficient of determination (R^2) into account to help us choose the equation that provided the best fit. According to (Workneh & Oke, 2013), a model with the highest R^2 value and the lowest values of χ^2, MBE, and RMSE is considered to have a good fit. These parameters can be calculated as follows:

$$\chi^2 = \sum_{i=1}^{N} (MR_{pre} - MR_{exp})^2 \frac{1}{N-n} \quad (10)$$

$$MBE = \frac{\sum_{i=1}^{N} (MR_{pre.} - MR_{exp})}{N} \quad (11)$$

$$RMSE = \sqrt{\frac{\left[\sum_{i=1}^{N} (MR_{pre.} - MR_{exp.})^2\right]}{N}} \quad (12)$$

Where MR_{exp} is the experimental moisture ratio (dimensionless), MR_{pre} is the predicted moisture ratio (dimensionless), N is the number of observations, and n is the total number of model constants.

2.2.5. Thermodynamic Parameters

Heating Capacity (Q_h) and Coefficient of Performance (COP) of TE Heat Pump

The heating capacity can be expressed hourly using the following Eq. (13).

$$Q_h = m_{ah} C_{pa} (T_h - T_{o,db}) \quad (13)$$

Where: Q_h is heating capacity, kWh, and C_{pa} is the specific heat of air (kJ/kg·°C),m_{ah} is the hot air flow rate, kg s^{-1}, T_h and $T_{o,db}$ are the temperature of the hot air at the outlet and the ambient temperature,°C respectively.

The equation for COP is given by:

$$COP = \frac{Q_h}{P} \quad (14)$$

Where P is the energy input to the TE drying system.

$$P = P_{TE} + P_{hb} + P_{cb} \quad (15)$$

Where: P_{cb} and P_{hb} are the blower energy of the cold and hot sides, kWh, respectively, and P_{TE} is the energy input to the TE modules, kWh.

Energy consumption for drying sliced tomato (E_T)

The total energy consumed by a 1kg batch of sliced tomato samples in the dryer, under different air velocities and slice thicknesses (ranging from 0.5 to 2.5 m/s and thicknesses of 0.5, 1, and 1.5 cm), is presented in Equation (16) (Koyuncu et al., 2007); and (Afolabi et al., 2014).

$$E_T = A V \rho_a Cp_a (T_{i,db} - T_{o,db})\, dt \quad (16)$$

Where: E_T is the total energy consumption per batch (kWh); A is the rack area (m^2); V is the air velocity (m/s); ρ_a is the air density (kg/m^3); dt is the total drying time per batch (h); $T_{i,db}$ is the dry-bulb temperature inside the drying chamber (°C); $T_{o,db}$ is the dry-bulb temperature outside the drying unit (°C); and C_{pa} is the specific heat of air (kJ/kg·°C).

Specific energy consumption (E_{sp})

The specific energy consumption is expressed by Eq. (17) according to (Koyuncu et al., 2007);and (Afolabi et al., 2014).

$$E_{sp} = \frac{E_T}{M_o} \quad (17)$$

Where E_{sp} is specific energy consumption (kWh/ kg), and Mo is the initial sample mass (kg).

Specific energy consumption (SEC)

The energy necessary to eliminate 1 kg of moisture from the product during the drying process is determined using the following calculation.

$$SEC = \frac{E_T}{m_w} \quad (18)$$

Where *SEC* is the specific energy consumption (kWh/kg), and m_w is the amount of moisture removed from the product (kg).

Energy Efficiency (η_E)

Energy efficiency, calculated by Eq. (19), is obtained by dividing the energy required to evaporate moisture from the drying product by the total energy (E_t) consumed during the drying process.

$$\boldsymbol{\eta E = \frac{E_{evap}}{E_T \times 3600} \times 100} \quad (19)$$

Where $\boldsymbol{\eta_E}$ is the energy efficiency (%), and $\mathbf{E_{evap}}$ is the energy required to evaporate moisture from the product (kg/h).

Energy Required to Evaporate Moisture from Product (E_{evap})

The energy needed to remove moisture from the tomato fruit during the drying process in the specialized dryer was determined using Equation (20).

$$\boldsymbol{E_{evap} = m_w \times L.H.V} \quad (20)$$

Where L.H.V is the latent heat of vaporization of water, kJ/kg, and m_w is the moisture evaporated from the product (kg).

The latent heat of vaporization can be obtained from Eq. (21).

$$\boldsymbol{L.H.V = (7.33 \times 10^6 - 16\, T_{abs}{}^2)^{0.5}} \quad 273.16 \le T_{abs} \le 338.72$$

$$L.H.V = 2.503 \times 10^3 - 2.386\,(T_{abs} - 273.16) \quad (21)$$

$$337.72 \le T_{abs} \le 533.16$$

Electrical Energy Consumption

The energy consumption of an appliance is determined by its power rating and how long it operates. For drying with Heat Pump Humidification Technology (HPD), you can calculate the electrical energy usage using Equation (22).

$$\mathbf{E = P \times t} \quad (22)$$

$$\mathbf{p = I \times V = I^2 R} \quad (23)$$

Where E is electrical energy consumption, kWh, P is represents Electrical Power, Watts, I is the electric current, Amperes, V is the Potential Difference or voltage, Volts, R is (Resistance) The opposition to the flow of electric current and, ohms Ω, and t is time, hours.

2.2.6. Determination of Quality Parameters of Tomato Slices

Lycopene and β-Carotene Content

The procedure outlined by (Nagata & Yamashita, 1992) was utilized to assess the contents of lycopene and β-carotene. A one-gram portion of the dried sample was added to a test tube along with 16 mL of a

hexane/acetone mixture in a 6:4 v/v ratio and was vigorously shaken for 15 minutes. Subsequently, the hexane layer was extracted, and its absorbance was recorded at wavelengths of 453, 505, 663, and 645 nm using a UV-VIS spectrophotometer (Model SM1200, New Milcher, USA).

The concentrations of β-carotene and lycopene (mg per 100 mL of solvent) were calculated using the following equations, where A_{663}, A_{645}, A_{505}, and A_{453} are the absorbance values at 663, 645, 505, and 453 nm, respectively. The results were expressed as mg per 100 g of the sample.

$$\text{Lycopene} = -0.0458 \times A_{663} + 0.204 \times A_{645} + 0.372 \times A_{505} - 0.0806 \times A_{453} \quad (24)$$

$$\beta\text{-carotene} = -0.216 \times A_{663} - 1.220 \times A_{645} - 0.304 \times A_{505} + 0.452 \times A_{453} \quad (25)$$

Total Antioxidant Activity

The total antioxidant activity of 80% methanolic extracts from the dehydrated samples was assessed by their ability to scavenge the stable 1,1-diphenyl-2-picrylhydrazyl (DPPH) radical, as outlined by (ABE et al., 1998). In brief, we combined 1 mL of 0.5 mM DPPH in methanol with 2.0 mL of 100 mM sodium phosphate buffer (pH 5.5) and added 2.0 mL of methanolic extract at various concentrations. After thorough mixing, the solutions were incubated at room temperature in the dark for 30 minutes, and the absorbance was measured at 517 nm. The resulting antioxidant activity was expressed as:

$$\%\ \text{radical scavenging activity} = [1 - (A_{517\ \text{sample}} / A_{517\ \text{control}})] \times 100 \quad (26)$$

3. RESULTS AND DISCUSSION

3.1. CFD simulation results

CFD simulation was used to predict airflow distribution inside the drying chamber under different conditions, including with and without fans, varying outlet fan speeds, and different outlet hole areas. The simulation results showed good agreement with experimental data.

Figure 5 illustrates the air velocity streamline distribution inside the simulated drying chamber. The streamlines trace the airflow from the inlet, through the interior of the chamber, to the outlet under various cases:

- **Figure 5a** shows the airflow distribution without any fans. The airflow inside the chamber is poorly distributed with minimal circulation.
- **Figure 5b** displays the airflow with two small fans inside the drying chamber, which promotes better air agitation.
- **Figure 5c** shows the airflow with only an outlet fan, where the formation of air vortices begins inside the chamber.
- **Figure 5d** illustrates the airflow with both an outlet fan and two small fans inside the chamber, resulting in increased air movement and improved airflow distribution, enhancing the drying process.

(a) Without any fan	(b) With only two small inside fans	(c) With only outlet fan (0.5 m s^{-1})	(d) With outlet fan (0.5 m s^{-1}) & two small inside fans

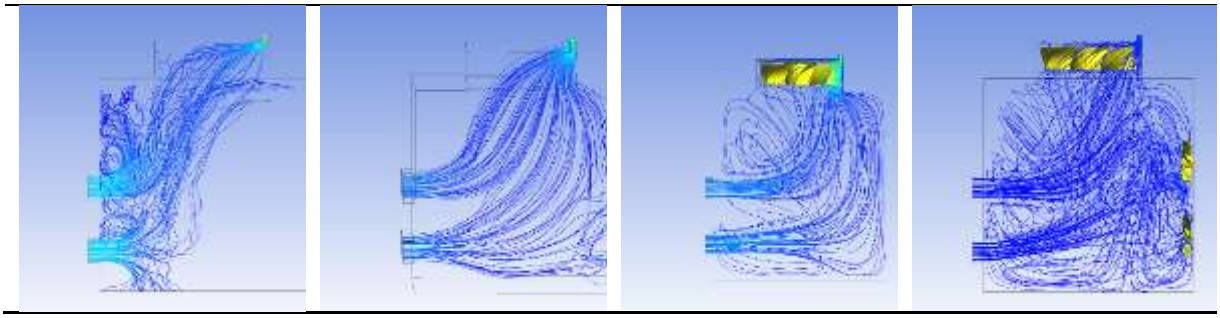

Figure 5. Air Velocity streamlines inside the drying chamber, Outlet hole area = 20 cm^2

Figure 6. Shows the air velocity streamlines distribution inside the simulated drying chamber with an outlet fan and two inside small fans in case of different outlet fan velocities (0.5, 1.5, 2, and 2.5 m s^{-1}). It illustrates that the airflow distribution in the case of the lower outlet fan velocity (0.5 m s^{-1}) was the best.

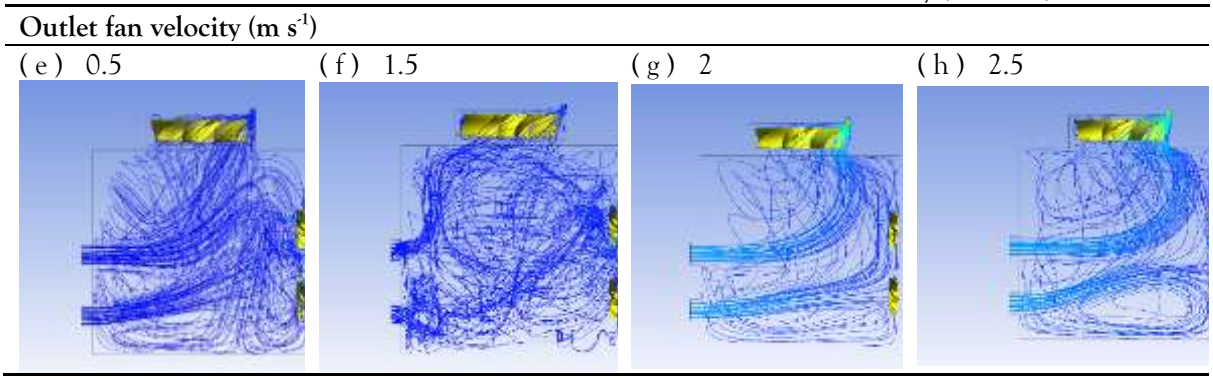

Figure 6. Air Velocity streamlines inside the drying chamber, Outlet hole area = 20 cm^2

Figure 7 shows the air velocity streamline distribution inside the simulated drying chamber with an outlet fan and two small internal fans for different outlet hole areas (20, 40, and 60 cm^2). The results illustrate that the airflow distribution was most uniform with the smallest outlet hole area (20 cm^2).

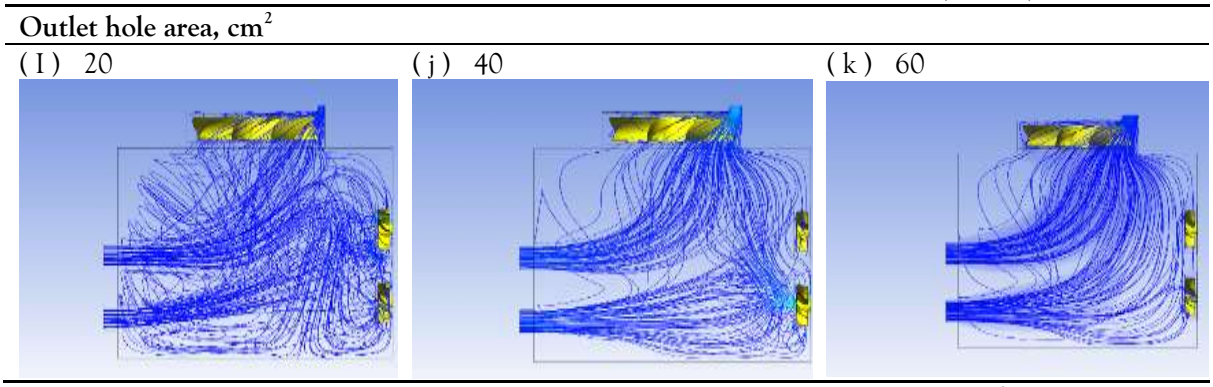

Figure 7 Air Velocity streamlines inside drying chamber, Outlet fan velocity = 0.5 m s^{-1}

3.2. Drying Kinetics

Moisture content

Figure 8 illustrates the variation of moisture content with drying time under different treatments. The results show that higher air velocities shorten drying time, while lower air velocities lead to higher final moisture content. Likewise, reducing the outlet fan area resulted in lower moisture content. Increasing the thickness of tomato slices decreased the rate of moisture evaporation and prolonged the drying process. Figure 8 presents the moisture content of tomato slices at three thicknesses (0.5, 1.0, and 1.5 cm), four air velocities (0.5, 1.5, 2.0, and 2.5 m/s), and three outlet fan areas (20, 40, and 60 cm^2). The lowest moisture content was achieved at an air velocity of 2.5 m/s with a 0.5 cm slice thickness and an outlet area of 20 cm^2.

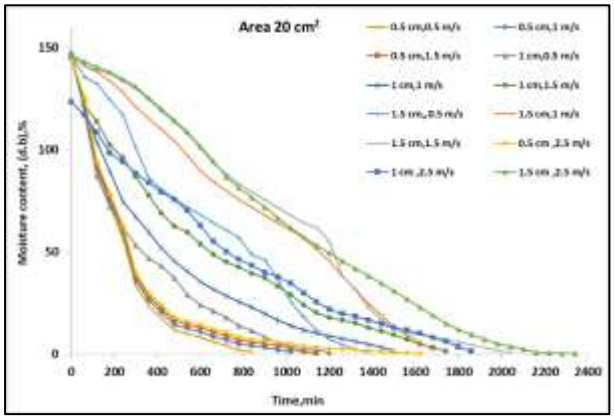

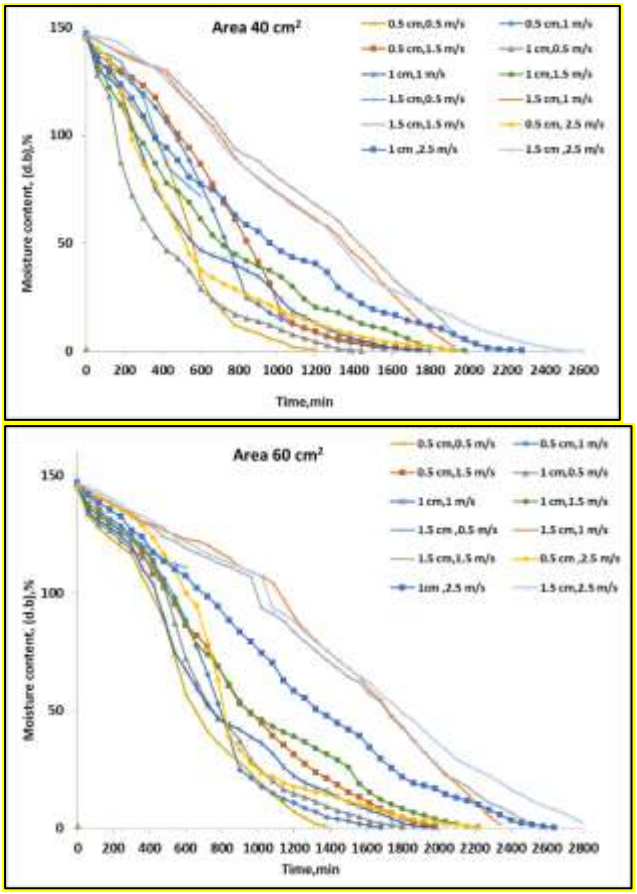

Figure 8. Effect of different drying treatments on moisture content

Drying Rate (DR) and Moisture Ratio (MR)

Drying rates of tomato slices with three thicknesses (0.5, 1, and 1.5 cm), four air velocities (0.5, 1.5, 2.0, and 2.5 m/s), and three outlet fan areas (20, 40, and 60 cm²) are presented in Figure 9. It is evident from Figure 9 that the lowest drying rate (0.00829 kg/h) was observed at an air velocity of 2.5 m/s with a 1.5 cm slice thickness and a 60 cm² outlet area. In contrast, the highest drying rate (0.02666 kg/h) occurred at 0.5 m/s air velocity with 0.5 cm slice thickness and a 20 cm² outlet area.

The data reveal that increasing both air velocity and slice thickness resulted in decreased drying rates. This is because greater slice thickness increases the amount of water and lengthens the vapor removal path, making moisture transfer through the product texture more difficult and thus prolonging drying time. Similarly, higher air velocities contributed to longer drying times. These findings are consistent with previous studies.

(Doymaz,2017).

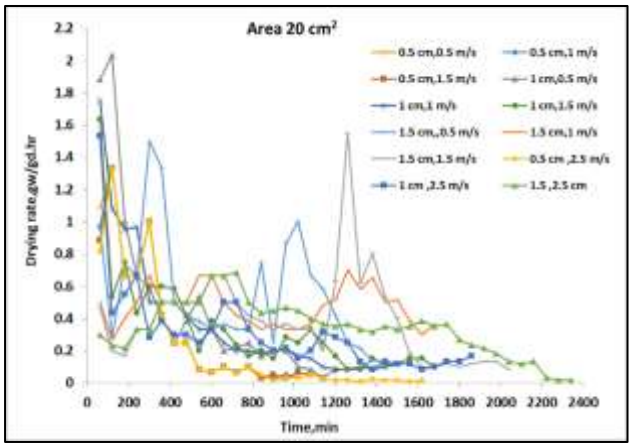

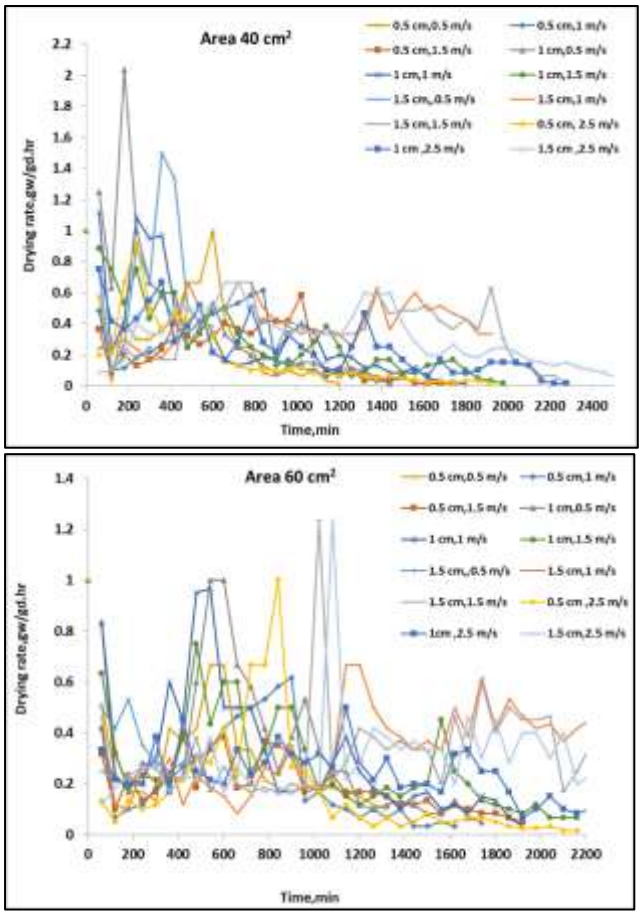

Figure 9. Effect of different drying treatments on drying rate

The variation of moisture ratio with drying time for drying tomato slices using a Thermoelectric Heat Pump with three thicknesses (0.5, 1, and 1.5 cm), four air velocities (0.5, 1.5, 2.0, and 2.5 m/s), and three outlet fan areas (20, 40, and 60 cm²) is presented in Figure 10.

In all treatments, the moisture ratio decreased steadily with increasing drying time. At the beginning, the rate of moisture removal was high due to the elevated initial moisture content. As drying continued, the evaporation rate gradually declined. In the final stage, the formation of a surface layer on the leather created resistance to water migration, further reducing the moisture ratio (Abbasi et al., 2010). Decreasing the air velocity from 2.5 m/s to 0.5 m/s and the tomato slice thickness from 1.5 cm to 0.5 cm leads to a rapid decrease in the moisture ratio, as depicted in Figure 10.

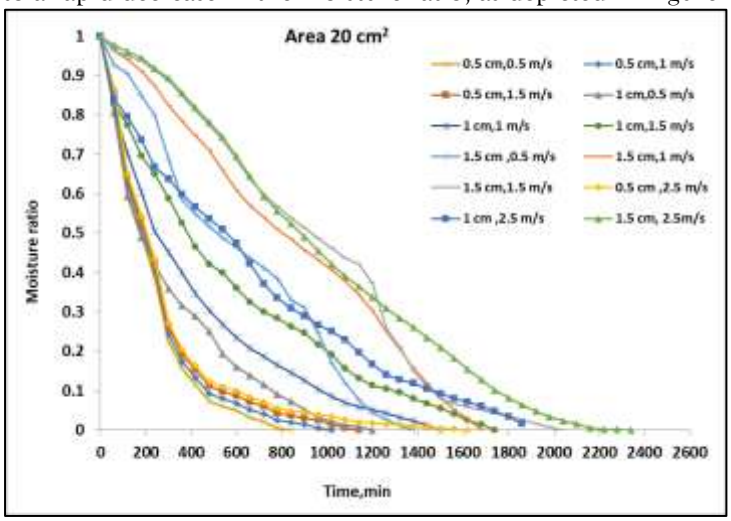

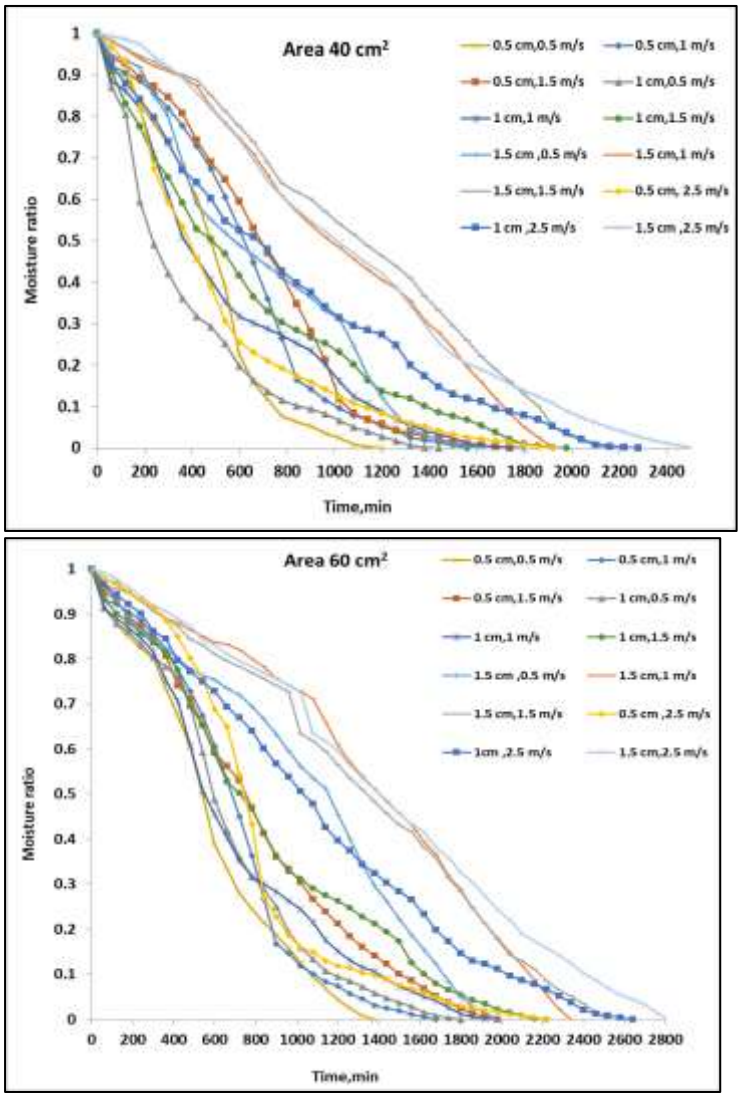

Figure 10. Effect of different drying treatments on moisture ratio .

Mathematical Modeling

Tables 1 and 2 present the drying behavior of tomato slices modeled using two selected mathematical approaches under varying air outlet areas, slice thicknesses, and air velocities. The results indicate that both models accurately described the drying behavior of tomato slices across all treatments. Based on higher R^2values and lower RMSE, MBE, and $\chi 2$, the Lewis model provided a better fit ($0.818 < R^2 < 0.996$, $0.001011318 <$ RMSE < 01.582627562, $-0.36809 <$ MBE < 1.335518, $0.000369 < \chi^2 < 0.630505$) as shown in Table 1.

Notably, the drying rate constant (k_L) exhibited a decreasing trend with increasing slice thickness, air outlet area, and air velocity.

Table 1. Statistical results of the fitted models (Lewis) for different outlet areas, slice thicknesses, and air velocities for tomato slices

Outlet fan area . cm^2	Slices thickness	Air velocity	$_1K$	RMSE	^2R	MBE	$^2\chi$	SE

	0.5	0.5	0.0055	0.0571488 4	0.981357	-0.03133	0.00381	0.042526
		1.5	0.0048	0.040036	0.9896992	-0.22587	0.001817	0.0302940 2
		2	0.0042	0.003919	0.9926746 8	-0.36809	0.000949	0.0252079
		2.5	0.0035	0.032049	0.9880392 4	0.110933	0.001067	0.0300348 1
	1	0.5	0.0035	0.0010113 2	0.9885052 1	-0.36380440 4	0.0008091	0.0314305 8
		1.5	0.0026	0.0017704 3	0.9961637 8	1.16687316 8	0.0003688 4	0.0175672 2
		2	0.0019	0.0050448 1	0.9888118 4	-0.1136833	0.0009702 6	0.0295333 5
		2.5	0.0016	0.0095384 1	0.9800943 4	-0.0151826	0.0017131 5	0.0388963 7
	1.5	0.5	0.0021	0.0810292 4	0.9241037 4	-0.01904102 2	0.0176637 5	0.0781295 7
		1.5	0.0013	0.4951163 9	0.9306755 8	-0.0154763	0.0141367 6	0.0691745
		2	0.0015	0.1997163	0.8716182 8	-0.00658	0.0352889 8	0.0986568 1
		2.5	0.0016	0.1139880 8	0.8926641 5	-0.0044206	0.036968	0.0900779 6
	0.5	0.5	0.0035	0.201026	0.844712	-0.01132	0.041002	0.111525
		1.5	0.0025	0.180999	0.8565227 7	-0.01031	0.036641	0.1055197 5
		2	0.0025	0.269588	0.8184883 1	-0.00768	0.051849	0.1189039 1
		2.5	0.0024	0.023134	0.9861000 3	-0.0245	0.004221	0.0324173 1
	1	0.5	0.0032	0.0096402 3	0.9903440 6	-0.05206470 7	0.0020534	0.0280398 7
		1.5	0.003	0.0766081 2	0.9363477 3	-0.0095489	0.0137525 1	0.0688154 8
		2	0.0024	0.0766081 2	0.9502214 1	-0.0095489	0.0137525 1	0.0611933 5
		2.5	0.0017	0.0723901 1	0.9522052 7	-0.0080276	0.0120606 1	0.0601312 4

	1.5	0.5	0.0021	0.1425074	0.9023926	-0.010556021	0.0284804	0.0884698
		1.5	0.0011	0.1189780	0.9100665	-0.0092915	0.0217110	0.0772076
		2	0.0014	0.3159898	0.8435128	-0.00381	0.0526457	0.1087552
		2.5	0.0014	0.2282200	0.9015564	-0.00384838	0.035632	0.0857475
60	0.5	0.5	0.0023	0.112948	0.900115	-0.01787	0.024622	0.090392
		1.5	0.0023	0.238309	0.8341696	-0.00903	0.630505	0.1149831
		2	0.0017	0.126512	0.9215930	-0.0084	0.022711	0.0776288
		2.5	0.0016	0.152202	0.9075925	-0.00993	0.025717	0.0838319
	1	0.5	0.0022	0.1427783	0.8916151	-0.010274038	0.0269665	0.0920286
		1.5	0.002	0.0926609	0.9393961	-0.009867881	0.0166342	0.0684449
		2	0.0016	0.1039127	0.9356664	-0.0075286	0.0175576	0.0698956
		2.5	0.0009	0.0503992	0.9630053	-0.019226	0.0077746	0.0506008
	1.5	0.5	0.001	0.1158262	0.8663960	-0.011265856	0.0207928	0.0926331
		1.5	0.0008	0.1825876	0.8467714	-0.0056928	0.0296196	0.0966553
		2	0.0009	0.1834603	0.8754277	-0.00469	0.0289989	0.0913224
		2.5	0.0009	0.2146776	0.8835745	-0.00342273	0.031995	0.0896390

Table 2. Statistical results of the fitted models (Henderson and Pabis) for different outlet areas, slice thicknesses, and air velocities for tomato slices

Slices thickness	Air ve-locity	α	k_h	RMSE	^2R	MBE	$^2\chi$	SE
0.5	0.5	**1.3164**	0.006	0.0571488	0.9721209	-0.0495645	0.0038103	0.0519668

	1.5	**1.1691**	0.005	0.046388	0.9873999 6	-0.1448	0.002439	0.0334567 4
	2	**1.0466**	0.004	0.003642	0.9925396 2	1.297541	0.000882	0.0255129 2
	2.5	**0.8637**	0.003	0.059706	0.9750347 9	0.032779	0.003702	0.0440716
1	0.5	**1.2007**	0.004	0.0504745 3	0.983231	-0.0714343 7	0.0020381 4	0.0377478
	1.5	**1.0751**	0.003	0.0400427 9	0.9903343 3	-0.0543070 6	0.0016702 3	0.0276831 3
	2	**1.1924**	0.002	0.0106113 1	0.9769154 8	-0.0642558 5	-0.0108329 7	0.0417772 6
	2.5	**1.2301**	0.002	0.0095384 1	0.9341485 1	-0.0160255 6	0.0087025 9	0.0690408
1.5	0.5	**1.7073**	0.003	0.2304257 9	0.8562364 7	-0.0100740 4	0.0502310 6	0.1092977 5
	1.5	**1.5289**	0.002	0.1275691 1	0.8366473 9	-0.0064701 9	0.0548670 6	0.1117029 9
	2	**2.1653**	0.002	0.1997163 2	0.7564322 9	-0.004523	0.0675545 1	0.1318368 4
	2.5	**2.5501**	0.002	0.0701214 8	0.7804304 2	-0.0036391 3	0.0600942 6	0.1209116 4
0.5	0.5	**2.3843**	0.005	0.130176	0.790254	-0.0086	0.060262	0.128605
	1.5	**2.1569**	0.003	0.123172	0.7983451 1	-0.0078	0.053843	0.1225945 1
	2	**2.6587**	0.003	0.135237	0.7530456 3	-0.00622	0.072785	0.1358662 2
	2.5	**1.3997**	0.003	0.065932	0.9571730 8	-0.01257	0.012031	0.0546725 5
1	0.5	**1.4192**	0.004	0.0402013 7	0.9699736 4	-0.0231179 5	0.0085628 6	0.0482962 5
	1.5	**1.8521**	0.003	0.0916410 9	0.9214517 9	-0.0109251 2	0.0173082 4	0.0756420 8

	2	**1.6749**	0.002	0.0334764	0.95881644	-0.01920737	0.0060096	0.05475878
	2.5	**1.8582**	0.002	0.13291775	0.88221521	-0.00654825	0.02214487	0.08913424
1.5	0.5	**2.1689**	0.003	0.32583367	0.81266069	-0.00656187	0.06511852	0.12078956
	1.5	**1.6033**	0.001	0.11621901	0.85294212	-0.01591645	0.02120755	0.08890944
	2	**2.5156**	0.002	0.59962246	0.67794252	-0.002782	0.09990057	0.14757783
	2.5	**1.3148**	0.002	0.46842919	0.73427717	-0.0027361	0.07313561	0.12864393
0.5	0.5	**1.8238**	0.003	0.226876	0.838764	-0.01107	0.049457	0.115744
	1.5	**2.248**	0.003	0.390003	0.74869236	-0.00649	0.076433	0.13856928
	2	**1.8817**	0.002	0.20585	0.8588171	-0.00659	0.036954	0.10103925
	2.5	**1.9492**	0.002	0.246635	0.84368183	-0.00667	0.041673	0.10336788
1	0.5	**1.9965**	0.003	0.29086896	0.7980195	-0.00653506	0.05493638	0.12153713
	1.5	**1.9127**	0.002	0.09568809	0.92145179	-0.01097981	0.0171777	0.07564208
	2	**1.9749**	0.002	0.20653678	0.84837425	-0.0054916	0.03489762	0.10170662
	2.5	**1.9914**	0.002	0.44863273	0.71901014	-0.00264033	0.06920681	0.13128983
1.5	0.5	**1.7739**	0.002	0.56433662	0.65115867	-0.00357183	0.10130835	0.15780696
	1.5	**1.7832**	0.001	0.33581221	0.639703	-0.0047031	0.05447594	0.13468873
	2	**1.7671**	0.001	0.28000256	0.68020486	-0.005603	0.04425912	0.12443988

	2.5	**1.7827**	0.001	0.32132182	0.65658804	-0.00474284	0.04788851	0.12463007

A comparison study of the two examined drying models (Lewis's and Henderson and Pabis's models) was conducted to assess the most appropriate drying model for simulating and describing the drying behavior of tomato slices within the studied range of experimental parameters.

Table (3) presents the overall average of the obtained coefficient of determination (R^2), RMSE, MBE, and $\chi^2$for the observed and the predicted moisture ratio of the studied models.

Table (3) The overall average of the obtained (R^2), RMSE, MBE, and $\chi^2$for the three studied drying models

Model	RMSE	R^2	MBE	χ^2	SE
Lewis	0.128554	0.918082	0.002551	0.038403	0.072692
Henderson and Babis	0.188356	0.843195	0.0196432	0.038504	0.095304

The results showed that all the models analyzed successfully captured the drying behavior of tomato leather slices. To find the best fit, a comparative analysis was done between the actual and predicted moisture ratios, utilizing various statistical indicators. The effectiveness of the thin-layer drying models was judged using parameters such as reduced chi-square (χ2), root mean square error (RMSE), mean bias error (MBE), and standard error (SE). A more accurate model would display higher R2 values along with lower χ2 and RMSE values. Thus, the correlation coefficient (R2), reduced chi-square (χ2), RMSE, and SE were used to assess how well the mathematical models represented the experimental drying data.(Shi et al., 2013).

Table 3 demonstrates that the Lewis model is preferred for accurately describing the drying behavior and predicting moisture changes in tomato slices when utilizing the Thermoelectric Heat Pump (TE). This preference is attributed to its superior average values of the determination coefficient R^2 (0.918082) and its lower RMSE (0.128554), MBE (-0.002551), χ^2 (0.038403), and SE (0.072692) compared to other models.

Drying time

Figure 11 illustrates the effect of drying air velocity, slice thickness, and air outlet area on the drying time of tomato slices. As shown, the longest drying time occurred at an air velocity of 2.5 m/s with a slice thickness of 1.5 cm and an air outlet area of 60 cm^2. Conversely, the shortest drying time was observed at 0.5 m/s air velocity with a 0.5 cm slice thickness and a 20 cm^2 outlet area. As expected, drying time significantly increases with higher air velocity and greater slice thickness.

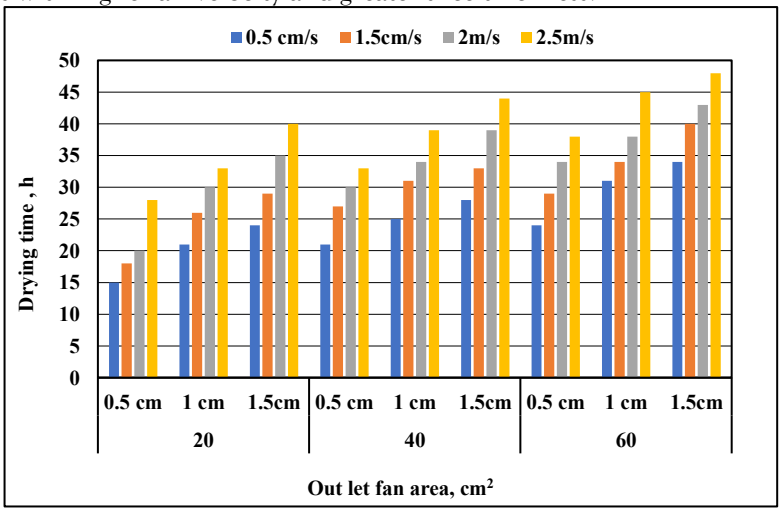

Figure 11. Drying time under different drying treatments.

As shown in Figure 11, the drying time was most affected at the smallest outlet area (20 cm^2) and least affected at the largest outlet area (60 cm^2), consistent with findings reported for carrot drying.(Ricce et

al., 2016) and banana drying (La Fuente & Tadini, 2018), where drying time increased with sample thickness. This can be attributed to surface hardening, higher water content, and a longer vapor diffusion path, all of which restrict moisture transfer within the product and consequently extend the drying time (Doymaz, 2017). An increase in air velocity from 0.5 m/s to 2.5 m/s and slice thickness from 0.5 cm to 1.5 cm at air inlet areas of 20 cm^2, 40 cm^2, and 60 cm^2 resulted in an increase in drying time by 166.67%, 109.52%, and 100%, respectively.

3.3. Thermal Performance of the Heat Pump Dehydrator

Heat Pump Performance

Table 4 presents the steady-state temperatures of the drying air and the hot side of the heat pump. The drying-air temperature reached 60 °C. The heating capacity attained a maximum value of 302 W, and the coefficient of performance (COP) at this drying-air temperature was 5.12.

Table 4. Drying-air temperature, hot-side temperature, heating capacity, power consumption of the hot-side blower, and COP for TE modules (ambient temperature: 25 °C).

Conditions	
Drying-air temperature (°C)	60 °C
Hot-side temperature (°C)	75°C
Heating capacity (W)	302 W
Hot-side blower power (W)	45 W
Power input to four TE Module (series arrangement)	13.95 W
COP	5.12

Energy Consumption for Drying Sliced Tomato (E_T)

From Figure 12, the maximum energy consumption (2.64 kWh) was recorded at an air velocity of 2.5 m/s with a slice thickness of 1.5 cm and an air outlet area of 20 cm^2. The minimum energy consumption (0.42 kWh) occurred at 0.5 m/s air velocity with 0.5 cm slice thickness and the same outlet area of 20 cm^2.

The average total energy requirement decreased due to increased heat transfer rates and greater water vapor pressure deficits in the drying samples, as well as enhanced convective hot air flow over the sample surface. Similar observations were made by (Routray & Rayaguru, 2012); and (Taghinezhad et al., 2021) , who concluded that total energy consumption during drying increases with both air velocity and slice thickness at constant air temperature, and decreases when these factors are reduced.

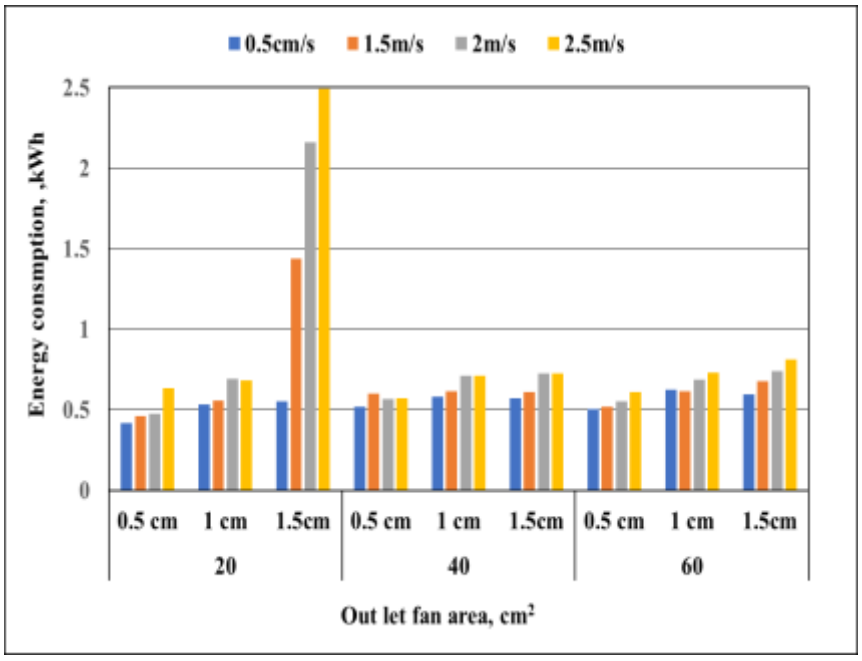

Figure 12. Energy consumption for drying sliced tomato under different drying treatments.

Specific energy consumption (E_{sp})

Specific energy consumption (E_{sp}) for sliced tomato samples at various slice thicknesses and air velocities under different air outlet areas is presented in Figure 13. The results show that E_{sp} increases with both air velocity and slice thickness. This trend is due to the longer time required for thicker slices to diffuse internal moisture to the surface before convective air can evaporate it, thereby prolonging the drying process and increasing energy usage.The maximum E_{sp} value (2.54 kWh/kg) was recorded for slices with a thickness of 1.5 cm at an air velocity of 2.5 m/s. At constant slice thickness, E_{sp} also increased with higher air velocities for the same fan outlet area. The minimum E_{sp} value (0.43 kWh/kg) was obtained for 0.5 cm thick slices at an air velocity of 0.5 m/s and an air outlet area of 20 cm².

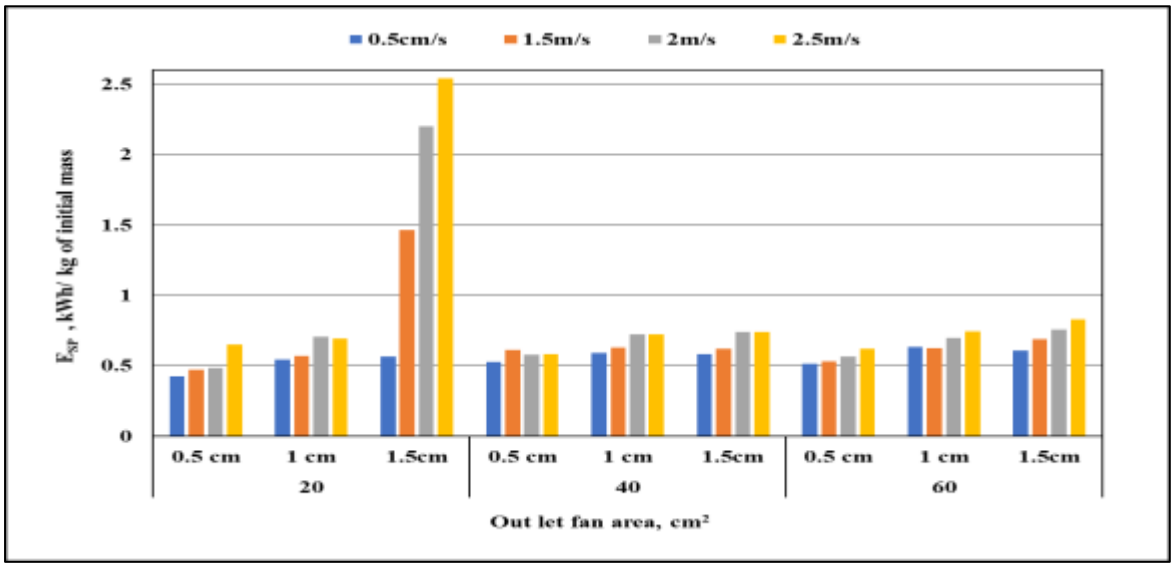

Figure 13. Specific energy consumption for initial weight under different drying treatments.

This is because with increasing slice thickness, the total energy consumption, since specific energy consumption is calculated by dividing the total consumed energy by the constant initial sample weight, its value increases when drying conditions require more energy. In this study, SEC was determined by substituting the measured total energy consumption (from Equation 11) and the initial sample weight into Equation 12. These results are consistent with the findings of (Routray & Rayaguru, 2012);(Nwakuba, 2019); (Nwakuba et al., 2020); and (Taghinezhad et al., 2021), who reported that drying thicker sample layers at co; constant air temperature and varying air velocities increases both total and specific energy requirements. This is due to the additional time needed for thicker samples to transfer internal moisture to the surface before it can be evaporated by the convective airstream, thereby extending the drying duration and raising energy demands. Air velocity and slice thickness were found to have significant effects on the SEC of the solar-electric dryer.

The specific energy consumption (SEC) for drying tomato slices is shown in Table 5. The lowest SEC value (0.72 kWh·kg^{-1}) was observed at an air velocity of 0.5 m/s and a slice thickness of 0.5 cm with a 20 cm² air outlet area. In contrast, the highest SEC (4.28 kWh·kg^{-1}) was recorded at 2.5 m/s and a slice thickness of 1.5 cm with the same outlet area.

Table 5. Specific energy consumption for evaporated water under different drying treatments.

Outlet Area,cm²	Air velocity m/s	0.5	1.5	2	2.5
	Slice thickness,cm				
20	0.5	0.71933	0.796992	0.814975	1.094869
	1	0.912569	0.955028	1.183038	1.165462
	1.5	0.948158	2.466242	3.707692	4.280656
40	0.5	0.889463	1.034774	0.975604	0.985893

	1	0.995483	1.056854	1.218209	1.216454
	1.5	0.97818	1.045847	1.241783	1.246261
60	0.5	0.868255	0.893608	0.952542	1.04733
	1	1.066402	1.050694	1.174086	1.24918
	1.5	1.0255	1.160534	1.273676	1.393098

Increasing the slice thickness from 0.5 cm to 1.5 cm resulted in a higher SEC to slices requiring longer drying times, which directly increases the total energy consumption (E_T). Conversely, thinner slices facilitate faster moisture removal, thereby reducing both drying time and energy consumption.

With increased slice thickness, total energy consumption rises because the same amount of energy is divided by the lower moisture removal from the product. This combined effect—higher total energy use and reduced moisture removal—is a key factor in the increase of SEC (Taghinezhad et al., 2021). Similar results were reported by (Routray & Rayaguru, 2012), who observed that increasing slice thickness in microwave drying of kiwi fruit led to higher SEC values.

Energy Efficiency (η_E)

The energy efficiency (η_E) of the dryer at different air velocities, outlet areas, and slice thicknesses was calculated using Equation (16), and the results are shown in Figure 14. Energy efficiency decreased with increasing air velocity and slice thickness. Thinner slices promote a greater moisture gradient within the product, enabling more moisture removal in less time, which shortens drying duration and improves efficiency.

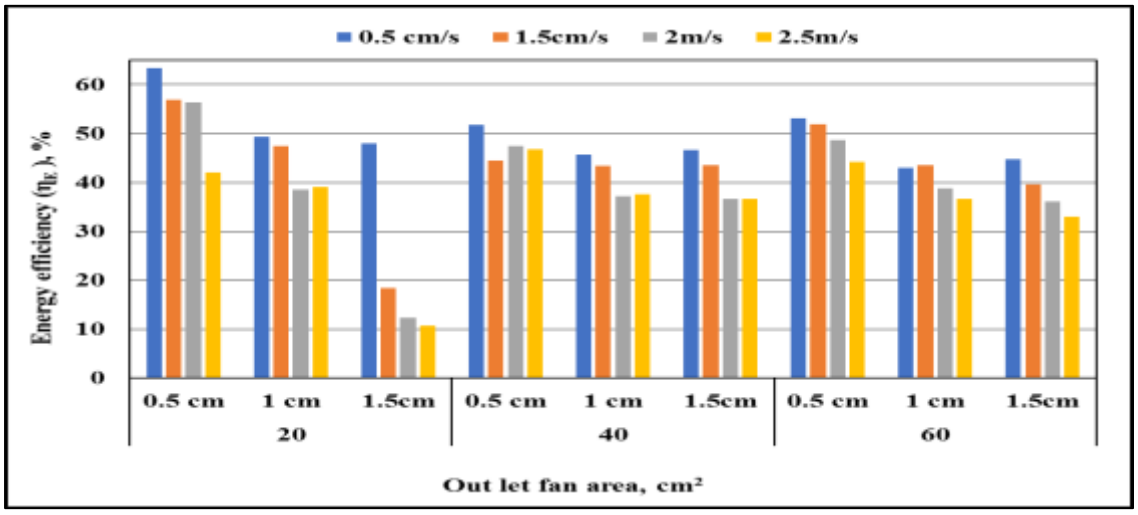

Figure 14. Energy Efficiency under different drying treatments

The lowest energy efficiency (10.67%) was observed at a slice thickness of 1.5 cm and an air velocity of 2.5 m s^{-1} with a 20 cm^2 air outlet area. In contrast, the highest value (63.4%) occurred at a slice thickness of 0.5 cm and an air velocity of 0.5 m s^{-1} under the same outlet area. These findings are consistent with those reported by (Sarsavadia, 2007); and (Motevali et al., 2014)

Energy efficiency is defined as the ratio of the energy used to evaporate moisture from the product to the total energy consumed during drying. Increasing slice thickness reduced energy efficiency because part of the heat energy was spent raising the temperature of the tomato slices to overcome the energy barrier caused by the longer capillary distance and to initiate mass diffusion. This left less heat available for surface moisture evaporation, resulting in lower efficiency. Conversely, reducing slice thickness increased energy efficiency values (Azadbakht et al., 2017); (Taghinezhad et al., 2021).

Drying tomato slices at lower air velocities increased the contact time between air and the material, allowing more moisture evaporation compared to higher velocities. Similar trends were reported by (Aviara et al., 2014) for tray drying of cassava starch and by (Azadbakht et al., 2017) for eggplant drying in a fluidized bed dryer.

Electrical Energy Consumption (P)

Figure 15 presents the electrical energy consumption of the Peltier module. The maximum electrical energy consumption (0.6696 kWh) occurred at an air velocity of 2.5 m s^{-1} and a slice thickness of 1.5 cm (air outlet area: 20 cm^2). The minimum value (0.20295 kWh) was recorded at 0.5 m s^{-1} air velocity and 0.5 cm thickness (air outlet area: 20 cm^2).

Overall, total electrical energy consumption decreased due to a higher heat transfer rate and greater water pressure deficit within the drying samples, which, combined with more effective convective hot air flow across the surface, shortened drying duration.

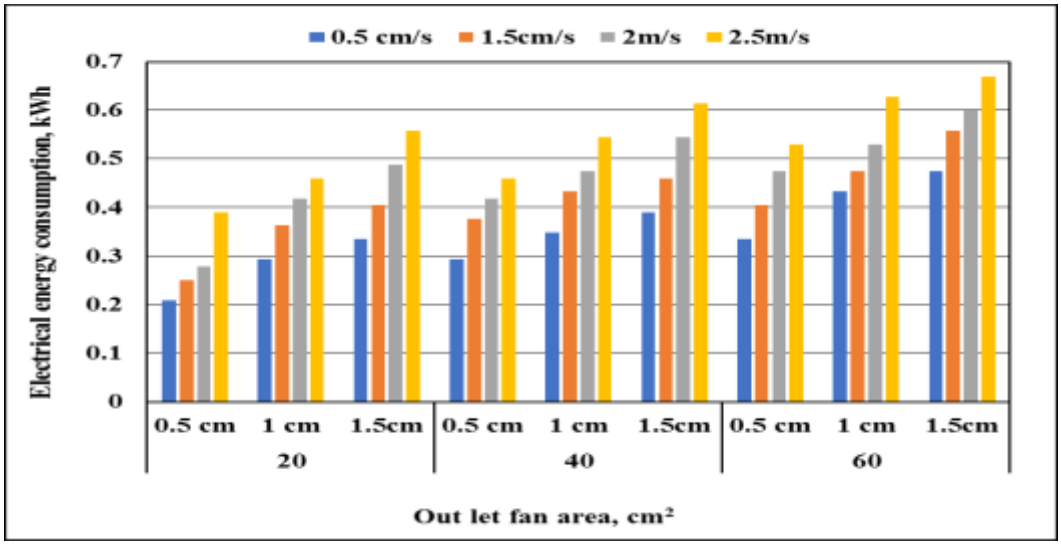

Figure 15. Electrical energy consumption by a (Thermo electric Heat pump for drying sliced tomato under different drying treatments.

3.4. Quality Parameters of Tomato Slices

Effects of Slice Thickness, Outlet Hole Area, and Air Velocity on Lycopene and β-Carotene

Figures 16 and 17 show that the contents of lycopene and β-carotene varied notably with changes in slice thickness, outlet hole area, and air velocity. The minimum lycopene content (9.72 mg/100 g) was recorded at a slice thickness of 1.5 cm and an air velocity of 2.5 m s^{-1} (outlet area: 60 cm^2), compared to 23.76 mg/100 g in fresh tomatoes. In contrast, the maximum lycopene content (52.46 mg/100 g) was obtained at a slice thickness of 0.5 cm and an air velocity of 0.5 m s^{-1} (outlet area: 20 cm^2), under elevated drying temperatures.

Similarly, β-carotene content followed a comparable trend. The lowest β-carotene content (3.85 mg/100 g) was observed at a slice thickness of 1.5 cm and an air velocity of 2.5 m s^{-1} (outlet area: 60 cm^2), whereas the highest value (8.94 mg/100 g) was recorded at a slice thickness of 0.5 cm and an air velocity of 0.5 m s^{-1} (outlet area: 20 cm^2). These results indicate that thinner slices, lower air velocities, and smaller outlet areas favor the retention of lycopene and β-carotene, likely due to reduced exposure time and less oxidative degradation during drying.

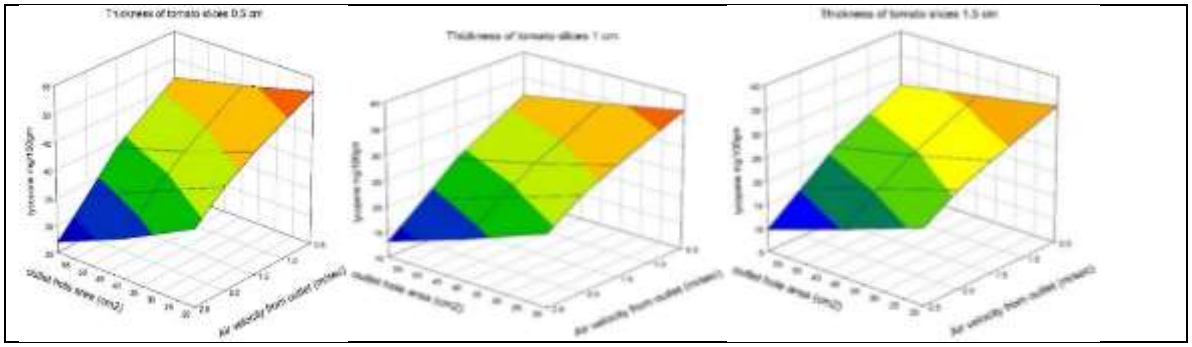

(A) (B) (C)

Figure 16. Response surface plots showing the effects of slice thickness (0.5, 1.0, and 1.5 cm) and outlet hole area at varying air velocities on lycopene content.

β-carotene contents in fresh tomatoes were 33.51 mg/100 g. Figure 18 illustrated the maximum value of β – carotene content was 93.35 mg/100 g at a tomato slice thickness of 0.5 cm and air velocity from the outlet (0.5 m s^{-1}) at outlet hole area 20 cm^2 when increased the temperature where the lowest value was 89.01 mg/100 g at tomato slice thickness 1.5 cm and air velocity from the outlet (2.5 m s^{-1}) at outlet hole area 60 cm2 at minimum temperature.

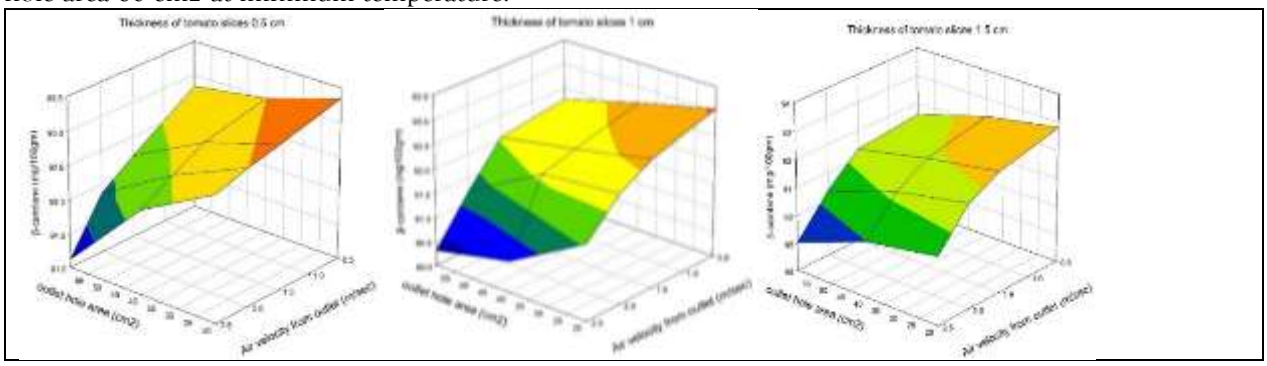

(A) (B) C)

Figure 17. Response surface plots showing the effects of slice thickness (0.5, 1.0, and 1.5 cm) and outlet hole area at varying air velocities on β-carotene content.

Our results are consistent with previous studies on tomatoes (Dauda, 2019) .The observed increase in lycopene content can be attributed to the drying process and temperature, which enhance the extractability of bioaccessible lycopene from the cellular matrix. Heat treatment promotes the conversion of cis-lycopene isomers to the more stable trans form, improving its bioavailability and thus increasing its measured concentration. Similar findings have been reported, showing that lycopene and β-carotene contents in tomato slices increase significantly after drying, with the highest values recorded for samples dehydrated at 50 °C; however, at 60 °C, the values started to decline (Dauda, 2019) . Another study reported that lycopene content increased significantly when slices were dried at 50 °C (48.9 ± 1.66 mg/100 g) and 60 °C (49.1 ± 1.09 mg/100 g), but decreased at 65 °C (44.8 ± 1.64 mg/100 g) and dropped further at 70 °C (31.8 ± 2.53 mg/100 g) (Das Purkayastha et al., 2013)

Effects of Tomato Slice Thickness, Fan Outlet Area, and Air Velocity on Antioxidant Activity

The antioxidant activity of fresh tomato was 81.73%, which decreased after drying under all tested conditions. As shown in Figure 18, the maximum post-drying antioxidant activity (30.37%) was observed at a slice thickness of 1.5 cm, an air velocity of 2.5 m s^{-1}, and an outlet area of 60 cm^2. Conversely, the minimum value (24.25%) was recorded at a slice thickness of 0.5 cm, an air velocity of 0.5 m s^{-1}, and a fan outlet area of 20 cm^2.

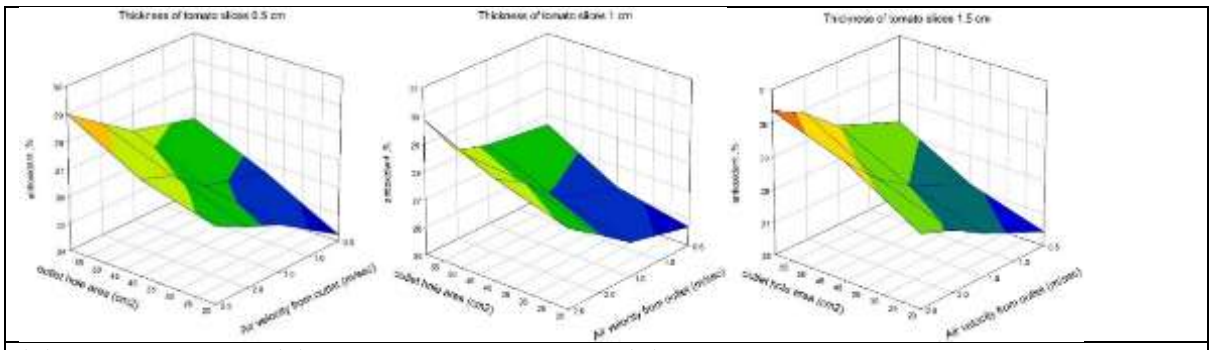

(A) (B) (C)

Figure 18. Response surface plots showing the effects of slice thickness (0.5, 1.0, and 1.5 cm) and outlet hole area at varying air velocities on antioxidant activity.

The trend in our results aligns with previously published findings for herbs (Azeez et al., 2019) . In fresh tomato slices, the antioxidant activity was 78.82 ± 1.52%, which decreased to 52.02 ± 0.27% after 300

minutes of drying at 50 °C. The antioxidant activity of fresh and thermally treated herb slices showed a similar pattern. Compared with fresh tomatoes, herb slices thermally treated at all tested temperatures for 30 and 60 minutes, as well as for 90 minutes at 70 °C, exhibited a reduction in antioxidant activity.

For tomato slices, antioxidant activity similar to that of fresh samples was retained when they were thermally treated for 90 and 120 minutes at 50 °C and 60 °C, and for 120 minutes at 70 °C. However, a significant decrease in antioxidant activity was recorded for all tomato slices processed for 150 to 300 minutes at any temperature, compared with fresh herbs.

The antioxidant potential of tomatoes is attributed to their high content of phenolic compounds, ascorbic acid, and lycopene. However, the drying method used can greatly influence the concentration of these antioxidant components and, consequently, the overall antioxidant activity.

It was also found that dried herb slices contained substantial amounts of lycopene (253.6 ± 0.96 μg/g) and β-carotene (121.86 ± 0.53 μg/g), with an antioxidant activity of 13.58%. In contrast, fresh tomato slices contained higher lycopene levels (510.6 ± 21.1 μg/g) and β-carotene levels of 95.6 ± 3.3 μg/g, with a much higher antioxidant activity of 60.8 ± 0.2% (Muthal, 2019).

4. CONCLUSION

Optimization of energy for dryer using TE as the heating source was investigated using sliced tomato samples at varying parameters (slice thickness 0.5, 1, and 1.5 cm, air velocity 0.5, 1.5, 2, and 2.5 m s^{-1} and outlet fan area 20,40 and 60 cm^2). Data showed that, by increasing slice thickness and air velocity, the drying time, E_t, $E_{sp,}$ and SEC increased. Drying rate and energy efficiency (η_E) decreased by increasing slice thickness and air velocity. The lowest E_T and E_{sp} values were obtained at 0.5 cm thickness, air velocity of 0.5 m s^{-1}, and fan outlet area of 20 cm^2. The lowest SEC value was obtained at 0.5 cm thickness, air velocity of 0.5 m s^{-1}, and fan outlet area of 20 cm^2. The highest value of η_E was 63.39 % at a slice thickness of 0.5 cm, 0.5 m s^{-1} air velocity, and 20 cm^2 fan outlet area. The maximum values of lycopene contents and β – carotene was obtained at a slice thickness of 0.5 cm, 0.5 m s^{-1} air velocity, and 20 cm^2 fan outlet area. The lowest antioxidant value was obtained at a slice thickness of 0.5 cm, 0.5 m s^{-1} air velocity, and 20 cm^2 fan outlet area.

Author Contributions: Conceptualization, M.I.E., M.S.G., A.W.E., and Sh.El.S., methodology and investigation, M.S.G., M.I.E. and A.W.E.; writing-original draft preparation, M. S. G., Sh. El. S. and A.W.E.; primitive and final field experiments, M.I.E., M.S.G. and Sh.El.S.; writing-review and editing, M.I.E., M.S.G., A.W.E., and Sh. El. The authors have read and agreed to the published version of the manuscript.

Funding: This research received no external funding.

Acknowledgments: We thank Mohamed Ramdan and Ahmed El Shal for their cooperation in editing and reviewing this manuscript, and we thank our family members.

Conflicts of Interest: The authors declare no conflict of interest.

REFERENCES

Abbasi, S., Mousavi, S. M., & Mohebbi, M. (2010). Mathematical Modeling of Onion Drying Process Using Hot Air Dryer. *Iranian Food Science and Technology Research Journal*, *6*(3). https://doi.org/10.22067/ifstrj.v6i3.9106

ABE, N., MURATA, T., & HIROTA, A. (1998). Novel DPPH Radical Scavengers, Bisorbicillinol and Demethyltrichodimerol, from a Fungus. *Bioscience, Biotechnology, and Biochemistry*, *62*(4), 661–666. https://doi.org/10.1271/bbb.62.661

Afolabi, T. J., Tunde-Akintunde, T. Y., & Oyelade, O. J. (2014). Influence of Drying Conditions on the Effective Moisture Diffusivity and Energy Requirements of Ginger Slices. *Journal of Food Research*, *3*(5), 103. https://doi.org/10.5539/jfr.v3n5p103

Akpinar, E. K., Bicer, Y., & Yildiz, C. (2003). Thin layer drying of red pepper. *Journal of Food Engineering*, *59*(1), 99–104. https://doi.org/10.1016/S0260-8774(02)00425-9

Alibas, I. (2007). Energy Consumption and Colour Characteristics of Nettle Leaves during Microwave, Vacuum and Convective Drying. *Biosystems Engineering*, *96*(4), 495–502. https://doi.org/10.1016/J.BIOSYSTEMSENG.2006.12.011

AOAC (Association of Official Analytical Chemists) Washington, DC, U. (2023). *Official Methods of Analysis* (Vol. 22).

Arikan, M. F., Ayhan, Z., Soysal, Y., & Esturk, O. (2012). Drying Characteristics and Quality Parameters of Microwave-Dried Grated Carrots. *Food and Bioprocess Technology*, *5*(8), 3217–3229. https://doi.org/10.1007/s11947-011-0682-8

Arslan, D., & Özcan, M. M. (2011). Dehydration of red bell-pepper (Capsicum annuum L.): Change in drying behavior, colour and antioxidant content. *Food and Bioproducts Processing*, *89*(4), 504–513. https://doi.org/10.1016/J.FBP.2010.09.009

Aviara, N. A., Onuoha, L. N., Falola, O. E., & Igbeka, J. C. (2014). Energy and exergy analyses of native cassava starch drying in a tray dryer. *Energy*, *73*, 809–817. https://doi.org/https://doi.org/10.1016/j.energy.2014.06.087

Azadbakht, M., Torshizi, M. V., Ziaratban, A., & Aghili, H. (2017). Energy and exergy analyses during eggplant drying in a fluidized bed dryer. *Agricultural Engineering International: CIGR Journal*, *19*(3), 177–182.

Azeez, L., Adebisi, S. A., Oyedeji, A. O., Adetoro, R. O., & Tijani, K. O. (2019). Bioactive compounds' contents, drying kinetics and mathematical modelling of tomato slices influenced by drying temperatures and time. *Journal of the Saudi Society of Agricultural Sciences*, *18*(2), 120–126. https://doi.org/10.1016/j.jssas.2017.03.002

Beigi, M. (2016). Energy efficiency and moisture diffusivity of apple slices during convective drying. *Food Science and Technology (Brazil)*, *36*(1), 145–150. https://doi.org/10.1590/1678-457X.0068

Botelho, V. R., Monte, M. L., Pereira Filho, R. D., & Pinto, L. A. de A. (2025). Internet of Things (IoT): Operational automation in experimental and computational analyses of hop residues drying. *Journal of Food Engineering*, *401*, 112662. https://doi.org/https://doi.org/10.1016/j.jfoodeng.2025.112662

Botha, G. E., Oliveira, J. C., & Ahrné, L. (2012). Quality optimisation of combined osmotic dehydration and microwave assisted air drying of pineapple using constant power emission. *Food and Bioproducts Processing*, *90*(2), 171–179. https://doi.org/10.1016/J.FBP.2011.02.006

Cernîşev, S. (2010). Effects of conventional and multistage drying processing on non-enzymatic browning in tomato. *Journal of Food Engineering*, *96*(1), 114–118. https://doi.org/10.1016/j.jfoodeng.2009.07.002

Chero, M. J. S., Zamora, W. R. M., Chero, J. A. S., & Villarreyes, S. S. C. (2021). Application of the Computer Vision System to the Measurement of the CIE L*a*b* Color Parameters of Fruits. *Advances in Intelligent Systems and Computing*, *1213 AISC*(January), 341–347. https://doi.org/10.1007/978-3-030-51328-3_47

Chong, C. H., Figiel, A., Law, C. L., & Wojdyło, A. (2014). Combined Drying of Apple Cubes by Using of Heat Pump, Vacuum-Microwave, and Intermittent Techniques. *Food and Bioprocess Technology*, *7*(4), 975–989. https://doi.org/10.1007/s11947-013-1123-7

Darvishi, H. (2013). Mathematical Modeling, Moisture Diffusion, Energy consumption and Efficiency of Thin Layer Drying of Potato Slices. *Journal of Food Processing & Technology*, *04*(03), 4–9. https://doi.org/10.4172/2157-7110.1000215

Das Purkayastha, M., Nath, A., Deka, B. C., & Mahanta, C. L. (2013). Thin layer drying of tomato slices. *Journal of Food Science and Technology*, *50*(4), 642–653. https://doi.org/10.1007/s13197-011-0397-x

Dauda, A. (2019). Chemical and Microbiological Evaluation of Dried Tomato slices for Nigerian System. *Global Journal of Nutrition & Food Science*, *1*(5), 1–4. https://doi.org/10.33552/gjnfs.2019.01.000521

Doymaz, I. (2004). Pretreatment effect on sun drying of mulberry fruits (Morus alba L.). *Journal of Food Engineering*, *65*(2), 205–209. https://doi.org/10.1016/j.jfoodeng.2004.01.016

Doymaz, I. (2012). Evaluation of some thin-layer drying models of persimmon slices (Diospyros kaki L.). *Energy Conversion and Management*, *56*, 199–205. https://doi.org/10.1016/J.ENCONMAN.2011.11.027

Doymaz, İ. (2017). Drying kinetics, rehydration and colour characteristics of convective hot-air drying of carrot slices. *Heat and Mass Transfer/Waerme- Und Stoffuebertragung*, *53*(1), 25–35. https://doi.org/10.1007/s00231-016-1791-8

FAO. (2025). *FAOSTAT (2025) Crops and Livestock Products.* https://www.fao.org/faostat/en/#data/QCL

Fatouh, M., Metwally, M. N., Helali, A. B., & Shedid, M. H. (2006). Herbs drying using a heat pump dryer. *Energy Conversion and Management*, *47*(15–16), 2629–2643. https://doi.org/10.1016/j.enconman.2005.10.022

Hammami, M., Torretti, S., Grimaccia, F., & Grandi, G. (2017). Thermal and performance analysis of a photovoltaic module with an integrated energy storage system. *Applied Sciences (Switzerland)*, *7*(11). https://doi.org/10.3390/app7111107

Hernandez-Perez, J. G., Carrillo, J. G., Bassam, A., Flota-Banuelos, M., & Patino-Lopez, L. D. (2021). Thermal performance of a

discontinuous finned heatsink profile for PV passive cooling. *Applied Thermal Engineering*, *184*, 116238. https://doi.org/10.1016/J.APPLTHERMALENG.2020.116238

Kipchumba Cherono, Milindi Sibomana, T. S. W. (2018). Effect of infield handling conditions and time to pre-cooling on the shelf-life and quality of tomatoes Efeito das condições de manuseio no campo e do tempo antes do pré-resfriamento na. *Brazilian Journal of Food Technology*, *21*(1), 1–12.

Koyuncu, T., Tosun, I., & Pinar, Y. (2007). Drying characteristics and heat energy requirement of cornelian cherry fruits (Cornus mas L.). *Journal of Food Engineering*, *78*(2), 735–739. https://doi.org/10.1016/j.jfoodeng.2005.09.035

La Fuente, C. I. A., & Tadini, C. C. (2018). Ultrasound pre-treatment prior to unripe banana air-drying: effect of the ultrasonic volumetric power on the kinetic parameters. *Journal of Food Science and Technology*, *55*(12), 5098–5105. ttps://doi.org/10.1007/s13197-018-3450-1

Lister, C., Hedges, L. J., & Lister, C. E. (2005). *Nutritional attributes of tomatoes*. https://www.researchgate.net/publication/268516162

Liu, D., Zhao, F.-Y., & Tang, G.-F. (2008). Modeling and Performance Investigation of a Closed-Type Thermoelectric Clothes Dryer. *Drying Technology*, *26*(10), 1208–1216. https://doi.org/10.1080/07373930802306995

Mai Al-Dairi. (2021). Effect of storage conditions on postharvest quality of tomatoes. *Journal of Agriculture and Marine Sciences* , *26*(1), 13–20. https://doi.org/10.24200/jams.vol26iss1pp13-20

Minaei, S., Chenarbon, H. A., Motevali, A., & Arabhosseini, A. (2014). Energy consumption, thermal utilization efficiency and hypericin content in drying leaves of St John's Wort (Hypericum Perforatum). *Journal of Energy in Southern Africa*, *25*(3), 27–35. https://doi.org/10.17159/2413-3051/2014/v25i3a2655

Monday John, F., Ayoola Patrick, O., & Adewale Moses, S. (2020). Effect of maturity stage on quality and shelf life of tomato (lycopersicon esculentum mill) using refrigerator storage system. *Eurasian Journal of Agricultural Research*, *4*(1), 23–44. https://orcid.org/0000-0003-2080-0446

Motevali, A., Minaei, S., Banakar, A., Ghobadian, B., & Darvishi, H. (2016). Energy analyses and drying kinetics of chamomile leaves in microwave-convective dryer. *Journal of the Saudi Society of Agricultural Sciences*, *15*(2), 179–187 https://doi.org/10.1016/j.jssas.2014.11.003

Motevali, A., Minaei, S., Banakar, A., Ghobadian, B., & Khoshtaghaza, M. H. (2014). Comparison of energy parameters in various dryers. *Energy Conversion and Management*, *87*, 711–725. https://doi.org/10.1016/J.ENCONMAN.2014.07.012

Mujumdar, A. S., & Menon, A. S. (2020). Drying of solids: principles, classification, and selection of dryers. In *Handbook of industrial drying* (pp. 1–39). CRC Press.

Muthal, T. (2019). Study on physiochemical quality characteristics of tomato slices dried using innovative drying system Harini R, Tejas Muthal, Chidanand DV and Sunil CK. ~ *4719* ~ *International Journal of Chemical Studies*, *7*(3), 4719–4723.

Nagata, M., & Yamashita, I. (1992). Method Tomato Masayasu * National NAGATA * and Ichiji YAMASHITA * of Vegetables rnamental Plants and Tea , Ministry of Agriculture , Forestry and Fisheries ,. *Forestry*, *39*, 1–4.

Nwakuba, N. R. (2019). Optimisation of energy consumption of a solar-electric dryer during hot air drying of tomato slices. *Journal of Agricultural Engineering*, *50*(3), 150–158. https://doi.org/10.4081/jae.2019.876

Nwakuba, N. R., Asoegwu, S. N., & Nwaigwe, K. N. (2016). Energy requirements for drying of sliNwakuba, N. R., Asoegwu, S. N., & Nwaigwe, K. N. (2016). Energy requirements for drying of sliced agricultural products: A review. Agricultural Engineering International: CIGR Journal, 18(2), 144–155.ced agricultural p. *Agricultural Engineering International: CIGR Journal*, *18*(2), 144–155.

Nwakuba, N. R., Chukwuezie, O. C., Asonye, G. U., & Asoegwu, S. N. (2020). Influence of process parameters on the energy requirements and dried sliced tomato quality. *Engineering Reports*, *2*(2). https://doi.org/10.1002/eng2.12123

Ochida, C. O., Itodo, A. U., & Nwanganga, P. A. (2018). A Review on Postharvest Storage, Processing and Preservation of Tomatoes (Lycopersicon esculentum Mill). *Asian Food Science Journal*, *6*(2), 1–10. https://doi.org/10.9734/afsj/2019/44518

Patel, V. K., Gluesenkamp, K. R., Goodman, D., & Gehl, A. (2018). Experimental evaluation and thermodynamic system modeling of thermoelectric heat pump clothes dryer. *Applied Energy*, *217*, 221–232.

https://doi.org/10.1016/J.APENERGY.2018.02.055

Perveen, R., Suleria, H. A. R., Anjum, F. M., Butt, M. S., Pasha, I., & Ahmad, S. (2015). Tomato (Solanum lycopersicum) Carotenoids and Lycopenes Chemistry; Metabolism, Absorption, Nutrition, and Allied Health Claims—A Comprehensive Review. *Critical Reviews in Food Science and Nutrition*, *55*(7), 919–929. https://doi.org/10.1080/10408398.2012.657809

Ricce, C., Rojas, M. L., Miano, A. C., Siche, R., & Augusto, P. E. D. (2016). Ultrasound pre-treatment enhances the carrot drying and rehydration. *Food Research International*, *89*, 701–708. https://doi.org/10.1016/J.FOODRES.2016.09.030

Routray, W., & Rayaguru, K. (2012). Mathematical modeling of thin layer drying kinetics of stone apple slices. *International Food Research Journal*, *19*, 1503–1510.

Saha, S. K., Dey, S., & Chakraborty, R. (2019). Effect of microwave power on drying kinetics, structure, color, and antioxidant activities of corncob. *Journal of Food Process Engineering*, *42*(4), 1–13. https://doi.org/10.1111/jfpe.13021

Sarsavadia, P. N. (2007). Development of a solar-assisted dryer and evaluation of energy requirement for the drying of onion. *Renewable Energy*, *32*(15), 2529–2547. https://doi.org/10.1016/J.RENENE.2006.12.019

Schiffmann, R. (2001). Microwave Processes for the Food Industry. In *Handbook of Microwave Technology for Food Applications* (pp. 299–377).

Shi, Q., Zheng, Y., & Zhao, Y. (2013). Mathematical modeling on thin-layer heat pump drying of yacon (Smallanthus sonchifolius) slices. *Energy Conversion and Management*, *71*, 208–216. https://doi.org/10.1016/J.ENCONMAN.2013.03.032

Sousa, W. A., Jr, A. M., Rodrigues, M. I., Engenharia, D. De, & Fea, D. A. (2004). Optimising a Microwave Assisted Banana Drying Process. *Proceeding of the 14th International Drying Symposium*, *August*, 1938–1945.

Taghinezhad, E., Kaveh, M., & Szumny, A. (2021). Thermodynamic and quality performance studies for drying kiwi in hybrid hot air-infrared drying with ultrasound pretreatment. *Applied Sciences (Switzerland)*, *11*(3), 1–17. https://doi.org/10.3390/app11031297

Tang, Y., Li, X., Xu, P., Yang, J., Zhang, Z., Wang, R., Zhao, D., & Elgamal, R. (2025). Performance Evaluation of a Solar-Assisted Multistage Heat Pump Drying System Based on the Optimal Drying Conditions for Solanum lycopersicum L. *Foods*, *14*(7), 121. https://doi.org/10.3390/foods14071195

Taylor, R. A., & Solbrekken, G. L. (2008). Comprehensive system-level optimization of thermoelectric devices for electronic cooling applications. *IEEE Transactions on Components and Packaging Technologies*, *31*(1), 23–31. https://doi.org/10.1109/TCAPT.2007.906333

Workneh, T. S., & Oke, M. O. (2013). Thin layer modelling of microwave-convective drying of tomato slices. *International Journal of Food Engineering*, *9*(1), 75–90. https://doi.org/10.1515/ijfe-2012-0205

Zalewska, M., Marcinkowska-Lesiak, M., & Onopiuk, A. (2022). Application of different drying methods and their influence on the physicochemical properties of tomatoes. *European Food Research and Technology*, *248*(11), 2727–2735. https://doi.org/10.1007/s00217-022-04081-0